DOT/FAA/TC-22/26

Federal Aviation Administration
William J. Hughes Technical Center
Aviation Research Division
Atlantic City International Airport
New Jersey 08405

Energy Management Algorithms and Displays

November 2022

Final report

U.S. Department of Transportation
Federal Aviation Administration

NOTICE

This report is available at the Federal Aviation Administration William J. Hughes Technical Center's Full-Text Technical Reports page: actlibrary.tc.faa.gov in Adobe Acrobat portable document format (PDF).

Technical Report Documentation Page

Form DOT F 1700.7 (8-72) Reproduction of completed page authorized

1. Report No.	2. Government Accession No.	3. Recipient's Catalog No.
DOT/FAA/TC-22/26		

4. Title and Subtitle	5. Report Date
Energy Management Algorithms and Displays	November 2022
	6. Performing Organization Code: ANG-E271

7. Author(s)	8. Performing Organization Report No.
Isaac Silver, Brian Kish, Markus Wilde	DOT/FAA/TC-22/26

9. Performing Organization Name and Address	10. Work Unit No. (TRAIS)
Florida Institute of Technology 150 W. University Blvd Melbourne, FL 32901	11. Contract or Grant No.: DTFACT-17-C-00001

12. Sponsoring Agency Name and Address	13. Type of Report and Period Covered
FAA Central Regional Office 901 Locust St Kansas City, MO 64106	Final Report 7/2/2018-7/31/2020
	14. Sponsoring Agency Code: AIR-714

Supplementary Notes

The Federal Aviation Administration William J. Hughes Technical Center Aviation Research Division COR was Robert McGuire
The Federal Aviation Administration Research Sponsors were Dave Sizoo, Flight Test Pilot, AIR-714 and Ross Schaller, Flight Test Engineer, AIR-714

16. Abstract

Loss of control at low altitude in the traffic pattern is one of the main causes of fatal accidents in general aviation. Many loss-of-control accidents can be attributed to the pilot losing awareness of the energy state of the aircraft. An intuitive and accessible display for energy state and specific excess power can potentially remedy these types of accidents. As general aviation aircraft are not equipped to measure a significant number of dynamic parameters, such a predictive energy display must be based on an algorithm running on a reduced set of parameters readily available from the current generation of light aircraft avionics. This paper discusses the challenges associated with designing a predictive projection-based or screen-based display for light aircraft and presents prototype solutions. Furthermore, the paper presents several energy state prediction algorithms and reports the flight test results producing the underlying aircraft performance database. The work presented has great potential of resulting in low-cost, easy-to-use, energy state prediction, warning and guidance displays based on available aircraft parameters.

17. Key Words	18. Distribution Statement
General Aviation - Energy Management General Aviation - Displays General Aviation - Stall Protection General Aviation - Loss of Control	This document is available to the U.S. public through the National Technical Information Service (NTIS), Springfield, Virginia 22161. This document is also available from the Federal Aviation Administration William J. Hughes Technical Center at actlibrary.tc.faa.gov.

19. Security Classif. (of this report)	20. Security Classif. (of this page)	21. No. of Pages	19. Security Classif. (of this report)
Unclassified	Unclassified	53	Unclassified

ACKNOWLEDGEMENTS

The team would like to thank the FAA for funding this effort. David Sizoo was the subject matter expert. Robert McGuire managed the program. Karen Mercer issued the contract. The team would like to thank Juan Merkt for his inputs. Finally, we would like to thank all the contract, admin, and aircraft support personnel who enabled the technical team to focus on the research.

Contents

Figures

Tables

Acronyms

Acronym	Definition
ADAHRS	Air Data/Attitude Heading and Reference System
AGL	Height Above Ground Level
AHRS	Attitude and Heading Reference System
APM	Aircraft Performance Model
CPU	Central Processing Unit
EAA	Energy Awareness Algorithm
EAS	Energy Awareness System
EASA	European Union Aviation Safety Agency
EMM	Energy Margins Model
FAA	Federal Aviation Administration
FIT	Florida Institute of Technology
GA	General Aviation
GPS	Global Positioning System
HMDI	High Definition Multimedia Interface
HUD	Heads-up Display
ISA	Standard Atmosphere
KIAS	Knots Indicated Airspeed
LCD	Liquid Crystal Display
LOC	Loss of Control
LRU	Line Replaceable Unit
MSL	Mean Sea Level
NTSB	National Transportation Safety Board
POH	Pilot Operating Handbooks
ROC	Rate of Climb
SRTM	Shuttle Radar Topography Mission
WAAS	Wide Area Augmentation System

Executive summary

Loss of control at low altitude in the traffic pattern is one of the main causes of fatal accidents in general aviation. Many loss-of-control accidents can be attributed to the pilot losing awareness of the energy state of the aircraft. An intuitive and accessible display for energy state and specific excess power can potentially remedy these types of accidents. As general aviation aircraft are not equipped to measure a significant number of dynamic parameters, such a predictive energy display must be based on an algorithm running on a reduced set of parameters readily available from the current generation of light aircraft avionics. This paper discusses the challenges associated with designing a predictive projection-based or screen-based display for light aircraft and presents prototype solutions. Furthermore, the paper presents several energy state prediction algorithms and reports the flight test results producing the underlying aircraft performance database. The work presented has great potential for low-cost, easy-to-use, energy state prediction, warning, and guidance displays based on available aircraft parameters.

1 Introduction

In the period 2012-2016, the National Transportation Safety Board (NTSB) recorded 6,397 accidents in general aviation (GA) in the U.S. alone, of which 19% (1,193) resulted in fatalities. This represents on average 73 fatalities per year, or one every five days. About 61% of the GA accidents occurred with fixed-wing aircraft flown for personal use. Of all fatal GA accidents, 46% can be attributed to inflight loss of control (LOC) (National Transportation Safety Board, 2019). Inflight LOC is defined by the NTSB as "loss of aircraft control while in flight, or extreme deviation from intended flightpath" (National Transportation Safety Board, 2011). In other words, a pilot is either distracted from the piloting tasks or is not paying sufficient attention to the airplane, leading to a significant loss in airspeed and/or altitude, resulting in a crash. A detailed look at the published NTSB accident data shows that 25% of all fatal accidents occur *en route*, at or around cruising altitude, whereas 35% occur during initial climb and approach, below 1000 ft in altitude. If a stall or spin starts at such low altitude, the pilot does not have enough altitude/time to recover the airplane and to convert altitude into airspeed before ground impact. This is highlighted by research conducted by the European Union Aviation Safety Agency (EASA). In 2008, EASA analyzed 57 stall/spin accidents and determined their exact locations; 10 of the accidents occurred between 1999-2008 and involved airplanes designed to be "spin resistant," namely Cirrus SR-20 and SR-22; the rest were fatal fixed-wing GA accidents occurring in 2006. The analysis found that 79% accidents happened at altitudes below 1000 ft, with 67% occurring within the traffic pattern (see Figure 1) (Hankers, et al., 2009). The data clearly show that focusing on stall and spin qualities of airplanes is too late in the mishap chain to prevent 35% of the total fatalities in fixed-wing, personal use GA.

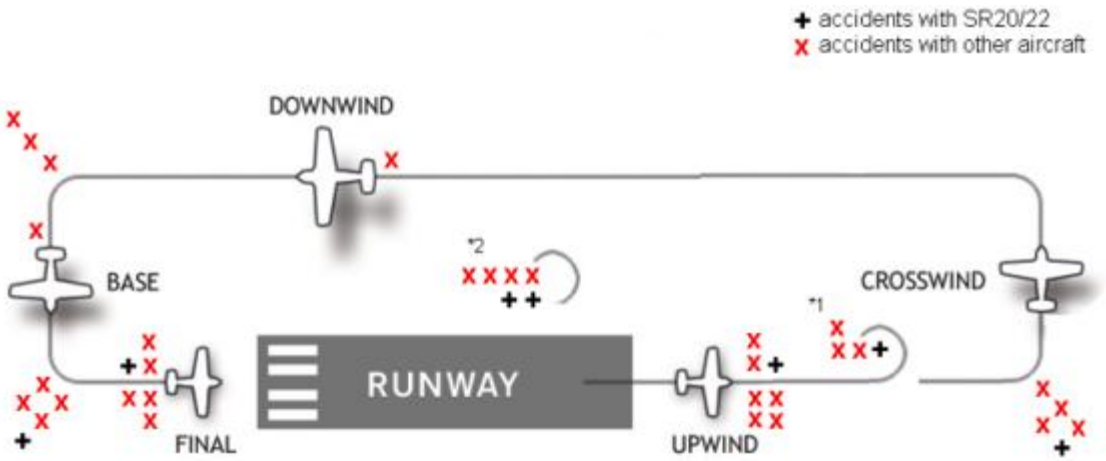

Figure 1. Positions of fatal stall/spin accidents within the traffic pattern

To counter the high number of LOC accidents at low altitudes, the Federal Aviation Administration (FAA) Small Aircraft Directorate has funded research to investigate countermeasures that address the problem "upstream" in the mishap chain. The team at Florida Institute of Technology (FIT) has been working with the FAA since 2017 in the areas of angle-of-attack and stall warning systems (Kish B. A., et al., March, 2018), the testing of stall characteristics of GA aircraft (Kish B. A., et al., June, 2018), the characterization of control forces and aircraft free response during flap configuration changes (Kish, Bernard, & Kimberlin, 2016; Kish B. A., et al., 2019), and the development of new means of compliance for low-speed flying qualities of Part 23 airplanes. Instead of using *idealized* data from flight simulations and numerical simulation models, these efforts were based on flight test data from typical production GA aircraft, with all the inherent limitations regarding data quality and availability. The experience gained in these efforts clearly showed that, to counteract LOC accidents upstream, flight energy management and hence flight energy awareness must be improved significantly.

The idea of using flight total energy management and energy awareness to improve aircraft performance and increase safety is not new. Rutowski (1954) proposed the use of total energy instead of altitude as independent display variable to enable a pilot to reach optimum performance. Zagalsky (1973) described instruments and systems for the optimal application of an aircraft's kinetic, potential, and chemical energy resources. Calise (1977) modeled altitude and flight-path angle dynamics for energy management solutions. Wu et al. (1994) developed a total energy control system for the optimization of the point-mass energy state. It was soon found that the application of total energy principles required integrated flight and propulsion controls (Lambregts A. A., 1983). Such a coordination of controls must be supported by purpose-designed flight displays (Amelink, Mulder, Van Paassen, & Flach, 2005), and by real-time

guidance displays to visualize the relationships between the flight dynamics variables and the current energy state (Lambregts, Rademaker, & Theunissen, 2008; Atuahene, Corda, & Sawhney, 2011). Merkt (2013) emphasizes the need for the incorporation of energy management into the flight training curriculum, to increase safety and efficiency.

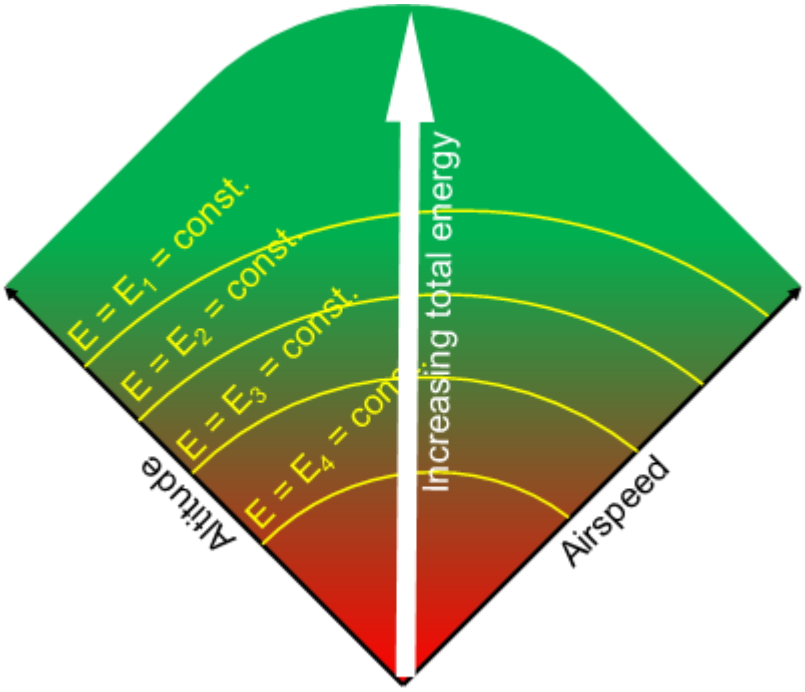

Figure 2. Energy funnel concept

Merkt (2013) also introduced the concept of the total energy funnel, for visualization of the energy management problem. The energy funnel shown in Figure 2 illustrates the total energy of an aircraft as combination of the kinetic energy (in terms of airspeed) and the potential energy (in terms of altitude). Within this funnel, there are arcs of constant total energy, on which altitude and airspeed can be exchanged without loss. The energy funnel also clearly illustrates the idea of energy reserves. If an aircraft is flying high and slow, a stall will not result in a catastrophe, as the potential energy can be converted into kinetic energy. If an aircraft flies low and fast, approaching obstacles can be avoided by converting kinetic energy into potential energy and climbing. The critical case is obviously low and slow, which is the condition aircraft inevitably go through in the traffic pattern. To use the energy funnel to generate energy awareness with pilots and to guide their decision-making process in case of impending loss of control, the cockpit must be equipped with energy management displays. These displays must inform the pilot in an intuitive and quickly accessible form about the current and projected energy state. If

the aircraft will exceed the limits of *healthy* kinetic, potential, or total energy within a set time, the pilot must be clearly warned and guided towards effective countermeasures. For the display to become an asset and not a nuisance or a burden, it must be designed carefully with minimization of display clutter and clear identification of critical information in mind.

Most of the research examples cited focus on increasing performance and efficiency of military and commercial, Part 25, aircraft. The field of general aviation, with significantly less sophisticated instrumentation, less experienced pilots, and less funding available to introduce new technologies, has not found as much attention. The research presented in this paper aims to close this knowledge and technology gap. The objective was the development of a heads-up display (HUD) for light GA aircraft, presenting the minimum necessary amount of information to create energy awareness. In nominal operations, this display is supposed to be used by the pilot to achieve peak performance and efficiency. When the energy state reaches critical levels, the HUD must alert pilots clearly and guide them towards quick and effective countermeasures. The paper also presents the algorithms developed to compute the current total, kinetic and potential energy state, to track the available specific excess power (P_S), and to compute a prediction of the current energy state with a fixed prediction horizon. The resulting HUD and the underlying algorithms must be practical for use as retrofit solution for GA aircraft, with the inherent limitations: space for projection systems, structural rigidity of the cabin, computing resources, air data, mass, and inertia properties.

Section 2 discusses design challenges and lessons learned specific to designing a HUD for use in light GA aircraft. Section 3 provides an overview of the (P_S) and total energy calculations underlying the HUD, and Section 4 describes how the baseline values for the power and energy models can be derived from the data published in pilot operating handbooks. Section 5 presents prototype power and energy awareness displays. Section 6 outlines the design elements of an Energy Awareness System. The flight test program is reported in Section 7. Section 8 discusses future work to be conducted using the Energy Awareness System. Section 9 concludes the paper and provides an overview of future research in this area.

2 HUD design for light aircraft

A HUD provides flight data to the pilot via an optical system that allows the pilot to keep their eyes outside of the aircraft with the information superimposed on real world visual cues. Traditional HUD systems are comprised of an image generator, a collimator, and an optical combiner that is semitransparent, allowing an image to be placed in the pilot's natural line of sight (Figure 3). The traditional HUD produces an image which is conformal to the outside

world, collimated and therefore focused at infinity and is bright enough to be daylight visible in all conditions. The HUD must also be mounted to prevent image shift or vibration induced jitter and placed so that the *eyebox*, or box in which the pilot's eyes must be located to view the image, is properly positioned for comfort.

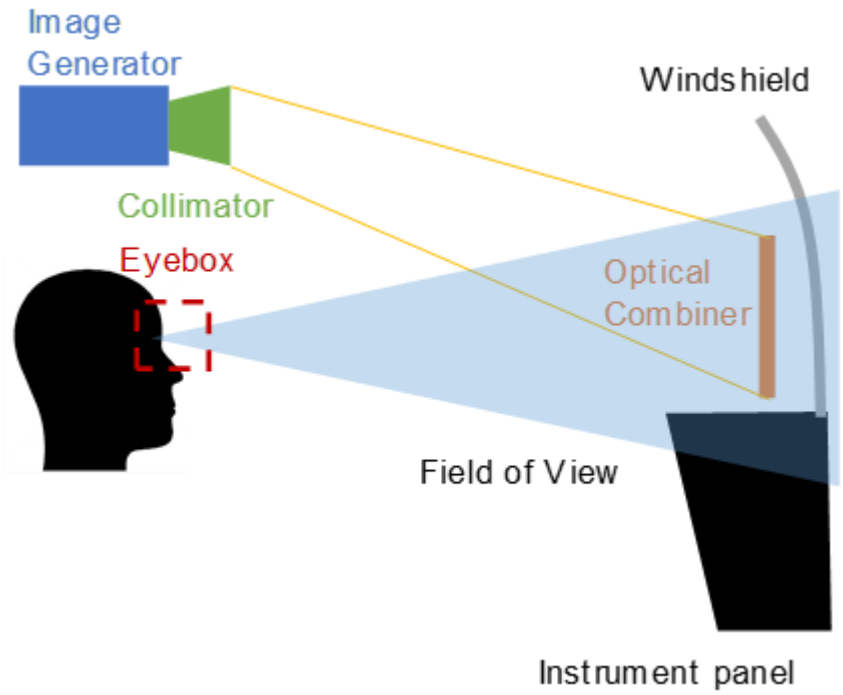

Figure 3. HUD system components

The typical optical system installed in large aircraft requires a series of transfer lenses and a long path length which allows the image to be projected on a flat combiner. Such systems are too large and heavy to be practically installed in light GA aircraft. To address these issues, the research HUD developed for the project presented here is designed to make use of a high intensity liquid crystal display (LCD) image generator and a single optical combiner (Figure 4) without the need for a complex lens system.

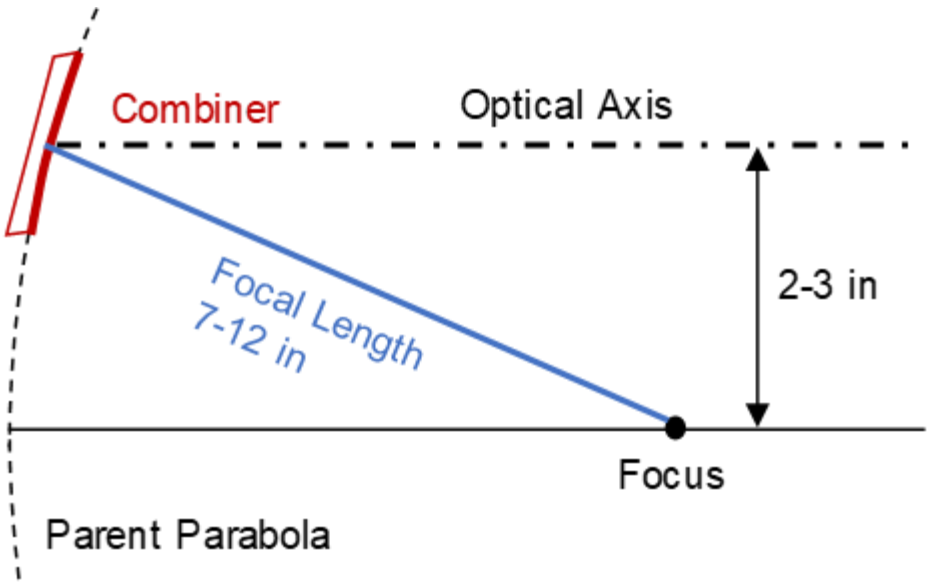

Figure 4. Combiner for conformal, collimated HUD

To generate a conformal, collimated image with a single element optical system, the combiner must be an off-axis paraboloid with a focal length of 7-12 inches with the optical axis offset vertically approximately 2-3 inches (Figure 4). With this optical combiner shape, the LCD image generator can be placed above the pilot, off axis from the pilot's line off site, and produce the required image to overlay the outside visual field. The optical combiner shape is specific to each unique mounting position for the HUD and thus is aircraft specific.

The research HUD is driven by a symbol generator built using a Raspberry PI general purpose computer. The flight data is collected directly from the data bus of a Garmin G5 flight instrument and includes attitude and heading reference system (AHRS) attitude data, air data, global positioning system (GPS), position, and velocity, and magnetometer derived heading. The HUD also receives acceleration data along the lateral and vertical axis. The image signal is then fed via a single micro high definition multimedia interface (HDMI) cable to a three inch, high intensity LCD display.

The basic information display includes attitude, indicated airspeed, barometric corrected altitude, heading, derived angle of attack, ground speed, and ground track. For this research, the general purpose nature of the symbol generator can be exploited to explore different display options that can be populated from the incoming data sources.

The research HUD was installed in a Cessna 172N and a Piper Warrior PA28-161 for testing. In the high-winged Cessna, the HUD was clipped into a temporary, GoPro style mount on the forward wing spar carry through structure just above and forward of the pilots head (Figure 5).

This proved to be a rigid and robust mounting point with little vibration transmitted from the airframe or the engine. The HUD structure was easily "detuned" from the vibration modes with small counterweights until it functioned at all power settings and airspeeds encountered during flight test.

Figure 5. Research HUD on a high-wing Cessna 172

The low-winged Warrior posed some additional challenges. The first attempt was to mount the HUD over the pilot in a similar position to the Cessna installation. The cabin top structure was easily disturbed by air loads and appeared to be excited by the engine vibration. Attempts to de-tune the HUD from the vibration modes of the cabin top were not successful. The second attempt was to mount the HUD to the glare shield with the projector off axis below the pilot's line of site. This setup proved to be more rigid, but the image was blurred by higher frequency vibrations that were amplified by the magnification of the optical system. De-tuning using counter weights produced a testable display, but further work needs to be done on the mount to match the performance of the HUD in the Cessna.

3 Specific excess power and total energy

The basic energy equation can be found in any Physics text book: total energy = potential energy + kinetic energy.

$$E = mgh + \frac{1}{2}mV^2 \qquad 1$$

The specific total energy is found by dividing by the weight:

$$\varepsilon = \frac{E}{mg} = h + \frac{1}{2g}V^2 \quad (2)$$

The specific excess power is found by taking the time derivative of the specific total energy:

$$P_s = \frac{d\varepsilon}{dt} = \frac{dh}{dt} + \frac{V}{g} \cdot \frac{dV}{dt} = \dot{h} + \frac{V}{g}\dot{V} \quad (3)$$

These equations provide instantaneous values of the aircraft state at any given time. To these equations, the aircraft is an inert point mass. There is no information on thrust or power setting. A simple way to estimate a future energy state after a prediction horizon τ is with the following equation:

$$\varepsilon_{future} = \varepsilon_{current} + P_{s_{current}}\tau \quad (4)$$

This tells the pilot what happens if the current P_s is held for a defined time interval τ, of 10 seconds.

The absolute total energy is not meaningful for flight. If the potential energy is measured with mean sea level (MSL) altitude, the airplane may hit the ground with positive potential energy. Similarly, the airplane will stall although having substantial kinetic energy. To feed an energy management display, it makes more sense to define the specific total energy reserve, comprising a potential energy component and a kinetic energy component.

The specific potential energy reserve for an airplane flying at pressure altitude h_p over terrain with ground altitude h_0 is equal to its above ground level altitude:

$$\varepsilon_{pot,res} = h_p - h_0 = h_{AGL} \quad (5)$$

The specific kinetic energy reserve is the difference between the indicated airspeed V_i and the stall speed V_S. As the stall speed varies as a function of the load factor n_z, the specific kinetic energy reserve is expressed as:

$$\varepsilon_{kin,res} = \frac{1}{2g}(V_i^2 - n_z V_s^2) \quad (6)$$

Estimates for the reserve energy components at prediction horizon τ are thus calculated by:

$$\varepsilon_{pot,res,future} = h_{AGL} + \dot{h}\tau \quad (7)$$

$$\varepsilon_{kin,res,future} = \frac{1}{2g}(V_i^2 - n_z V_s^2) + \frac{V_i}{g}\dot{V}\tau \quad (8)$$

The predicted specific energy reserve components still do not include any information on thrust or power setting. A pilot may like to know what happens if full throttle is set at the current condition (airspeed, altitude, temperature, n_z). In that case, the predicted energy becomes:

$$\varepsilon_{pot,res,future} = h_{AGL} + P_{s_{avail}}\tau \quad (9)$$

$$\varepsilon_{kin,res,future} = \frac{1}{2g}(V_i^2 - n_z V_s^2) + P_{s_{avail}}\tau \quad (10)$$

To get $P_{s_{avail}}$, we need a model for a given aircraft. Figure 6 shows examples for typical P_S curves.

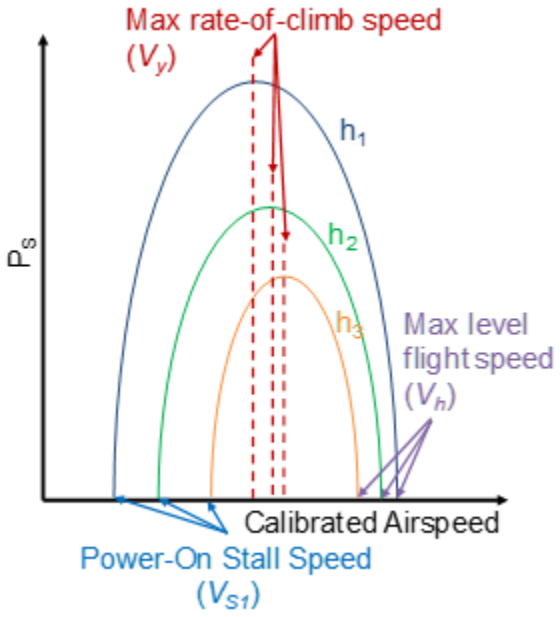

Figure 6. Typical P_s curves

The maximum available $P_{S,max}$ equals the maximum rate-of-climb (Max ROC) published in Pilot Operating Handbooks (POH) (Piper Aircraft Corporation, 1994). In examining POH data from Piper and Cessna, Max ROC changes linearly with respect to pressure altitude h_p and temperature deviation ΔT from the standard atmosphere (ISA). Therefore, simple scaling factors for $P_{S_{avail}}$ for changes in altitude and temperature can be derived directly from available POH data. Stall speed (V_s) and maximum level flight speed (V_h) can be scaled knowing n_z. Therefore, a P_s curve can be generated with x-axis crossings at V_s and V_h; and a vertex at optimum climb

speed V_y for maximum rate of climb ($V_{y,max}$). The P_s curve for all flight speeds, altitudes and temperatures can then be built using either a single parabola anchored at V_S on the left (less accurate because the second x-axis crossing is below V_h) or two parabolas that intersect at the vertex, with one parabola anchored at V_S and the second at V_h.

With the P_s curves known as a function of h_p, V_i, ΔT, n_z, V_s, V_h, and V_y, $P_{s_{avail}}$ can be computed for every instantaneous flight condition. The maximum $P_{s_{avail}}$ is with $V_i = V_y$ and $n_z = 1$.

4 Deriving specific excess power from pilot operating handbook

Figure 7 shows Max ROC information from Section 5 of the POH (Piper Aircraft Corporation, 1994). V_y is assumed to be constant 79 Knots Indicated Airspeed (KIAS) for all altitudes. The sea-level ROC for ISA $\left(ROC_{SL,ISA}\right)$ is 644 ft/min. This value, along with V_y, will be needed for the model.

MAXIMUM RATE OF CLIMB

ASSOCIATED CONDITIONS:
GROSS WEIGHT: 2440 lb.
POWER: FULL THROTTLE
MIXTURE: FULL RICH
FLAPS: UP
AIRSPEED: 79 KIAS

EXAMPLE
PRESSURE ALTITUDE: 5000FT
OAT: 16° C (ISA + 11° C)
MAX RATE OF CLIMB: 374 FPM

PRESSURE ALTITUDE FEET	OUTSIDE AIR TEMPERATURE				
	ISA - 15° C	ISA	ISA + 10° C	ISA + 20° C	ISA + 30° C
S.L.	677	644	624	604	585
1000	628	595	574	554	534
2000	578	545	524	504	485
3000	528	495	475	455	436
4000	478	446	425	405	386
5000	429	396	376	356	337
6000	379	346	326	306	287
7000	330	298	277	257	238
8000	280	248	227	207	188
9000	231	198	177	157	138
10000	181	149	128	108	89
11000	132	99	79	59	40
12000	83	49	29	9	-10
13000	33	0	-21	-41	-60

PIPER AIRCRAFT CORPORATION
PA-28-161, WARRIOR III
SECTION 5
PERFORMANCE

Figure 7. Max ROC information from Piper POH

A plot of the tabular data is shown in Figure 8. The temperature deviation from ISA only impacts the y-intercepts, but not the slopes. Thus, Max ROC drops 0.0496 ft/min for every 1 ft increase in pressure altitude.

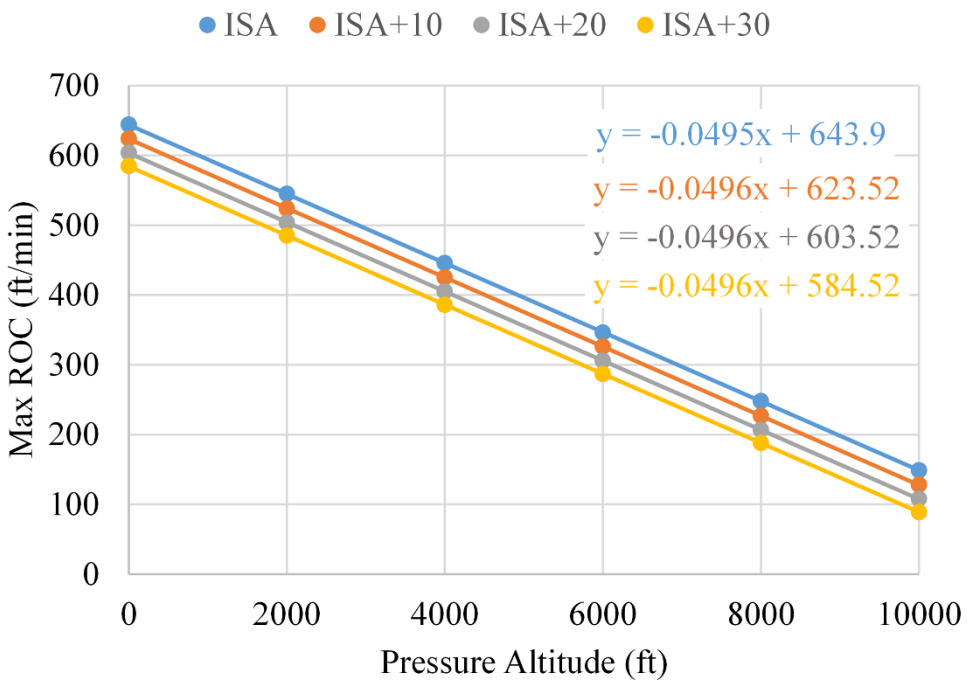

Figure 8. Max ROC versus pressure altitude

Figure 9 shows a plot of the y-intercepts (which correspond to Sea-level Max ROC) as a function of temperature deviation from ISA (ΔT). Sea-level Max ROC is a linear function of ΔT.

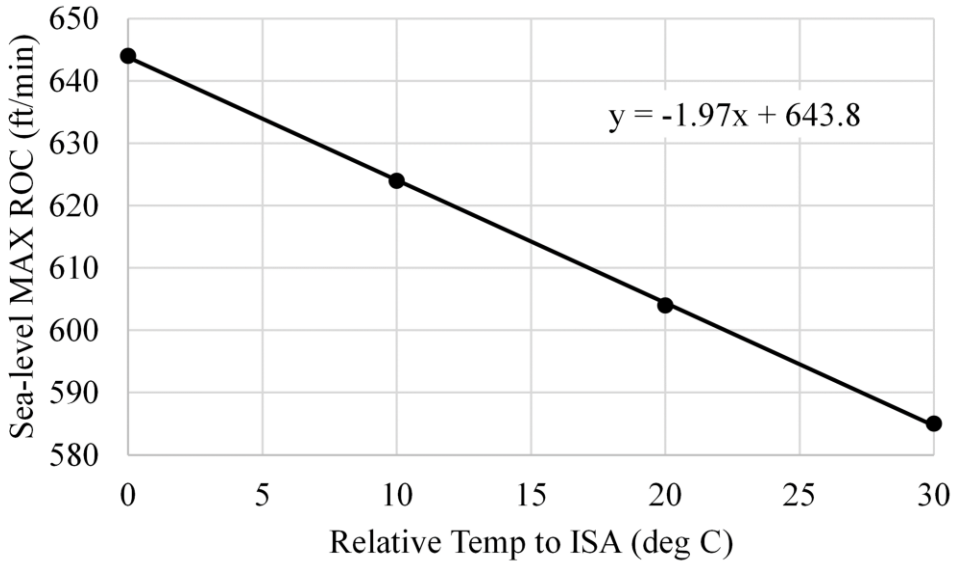

Figure 9. Sea-level Max ROC versus ΔT

With the maximum rate of climb at sea-level and ISA conditions, $ROC_{SL,ISA}$, given in the POH, Max ROC for any other altitude and temperature can be calculated with:

$$ROC_{max} = -0.0496 \cdot h_p + \left(-1.97\ \Delta T + ROC_{SL,ISA}\right) \tag{11}$$

Assume the P_S curve is a parabola, with the vertex at V_y and ROC_{max}. The general equation for a parabola with a horizontal shift V_y and a vertical shift ROC_{max} is:

$$y = k\left(x - V_y\right)^2 + ROC_{max} \tag{12}$$

Assume the parabola crosses the x-axis at V_S. It should also cross the x-axis at V_h, but we first assume it crosses at $\left[V_y + \left(V_y - V_s\right)\right]$. Then, we can solve for k assuming $x = V_s$ and $y = 0$:

$$k = \frac{-ROC_{max}}{\left(V_s - V_y\right)^2} \tag{13}$$

Thus, we get an equation for y (P_s) as a function of x (V_i) and ROC_{max}, which is a function of h_p and ΔT:

$$P_s = \frac{-ROC_{max}}{\left(V_s - V_y\right)^2}\left(V_i - V_y\right)^2 + ROC_{max} \tag{14}$$

Substituting for ROC_{max}, we get:

$$P_s = \frac{-\left[-0.0496\ h_p + \left(-1.97\ \Delta T + ROC_{SL,ISA}\right)\right]}{\left(V_s - V_y\right)^2}\left(V_i - V_y\right)^2 + \left[-0.0496\ h_p + \left(-1.97\ \Delta T + ROC_{SL,ISA}\right)\right] \tag{15}$$

Next, we account for n_z. If we assume that stall speed changes by a factor of $\sqrt{n_z}$ and ROC_{max} changes by a factor of $\frac{1}{n_z}$, then the equation for P_S becomes:

$$P_s = \frac{-\left[-0.0496\ h_p + \left(-1.97\ \Delta T + ROC_{SL,ISA}\right)\right]/n_z}{\left(V_s\sqrt{n_z} - V_y\right)^2}\left(V_i - V_y\right)^2 + \left[-0.0496\ h_p + \left(-1.97 \cdot \Delta T + ROC_{SL,ISA}\right)\right]/n_z \tag{16}$$

The parameters highlighted in yellow are constants found in the POH. The slopes highlighted in blue are found from linear fits of the POH climb data. The parameters highlighted in green are variables recorded in flight. If real-time temperature is unavailable, the work-around is to record ΔT from weather observations at the airport and to assume that it remains constant for the rest of the flight (at all altitudes).

Another option is to merge two parabolas that intersect at the vertex at V_y and ROC_{max}. The left side parabola is the previously derived parabola based on an x-axis crossing at V_s. The right side parabola has the x-axis crossing at V_h. As seen in Figure 10, V_h (Full Throttle) does change with altitude. The simplest option is to assume V_h is constant with altitude and use the sea-level value of $V_h = 117$ kts. Even at 6000 ft, this assumption would only result in a 2 kt error. The next simplest option is to assume a linear relation with altitude using the red line drawn. That would produce the following equation:

$$V_h = -\frac{3}{10{,}000} h_p + V_{h_{SL}} \qquad 17$$
$$= -\frac{3}{10{,}000} h_p + 117$$

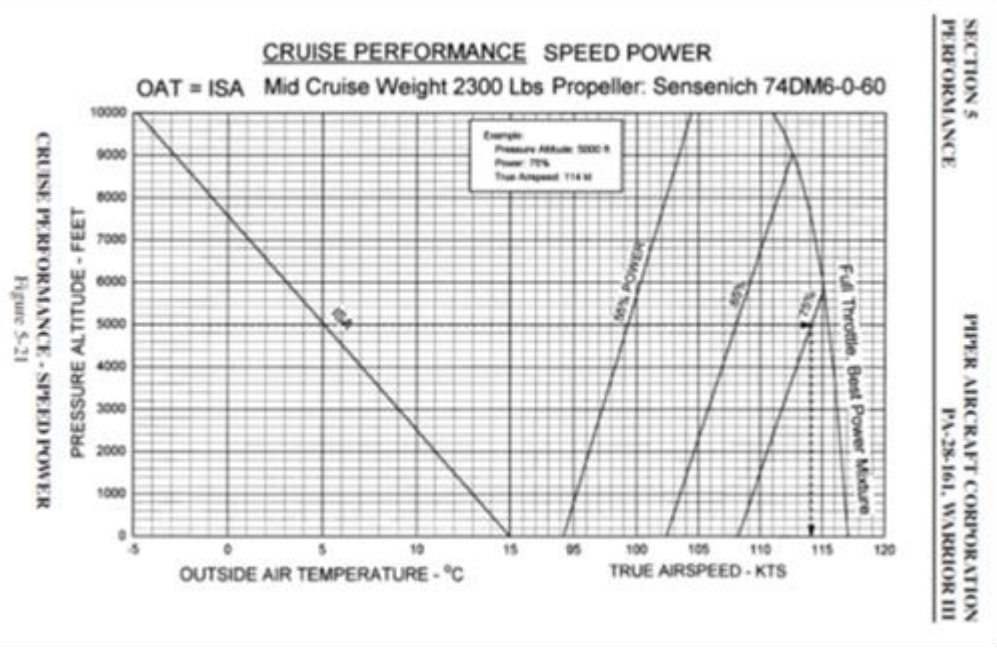

Figure 10. V_h versus pressure altitude from Piper POH

This linear model has only a 3 kt spread from sea level to 10,000 ft. It matches the actual curve up to 6,000 feet. It is within 1.5 kts up to 9,000 ft. The worst-case error is 3 kts at 10,000 ft.

The next consideration is how V_h changes with n_z. Based on recent constant-altitude turn performance data on a PA32, a scale factor of $\frac{1}{\sqrt{n_z}}$ is reasonable. Therefore, the equation for the right side parabola becomes:

$$P_s = \frac{-\left[-0.0496\ h_p + \left(-1.97\ \Delta T + ROC_{SL,ISA}\right)\right]/n_z}{\left[\left(-\frac{3}{10{,}000}h_p + V_{hSL}\right)\frac{1}{\sqrt{n_z}} - V_y\right]^2}\left(V_i - V_y\right)^2 + \left[-0.0496\ h_p + \left(-1.97\ \Delta T + ROC_{SL,ISA}\right)\right]/n_z \quad (18)$$

Again, the parameters highlighted in yellow are constants found in the POH. The slopes highlighted in blue are found from linear fits of the POH data. The parameters highlighted in green are variables recorded in flight. Figure 11 shows the P_s curves this equation produces for various combinations of h_p, ΔT, and n_z.

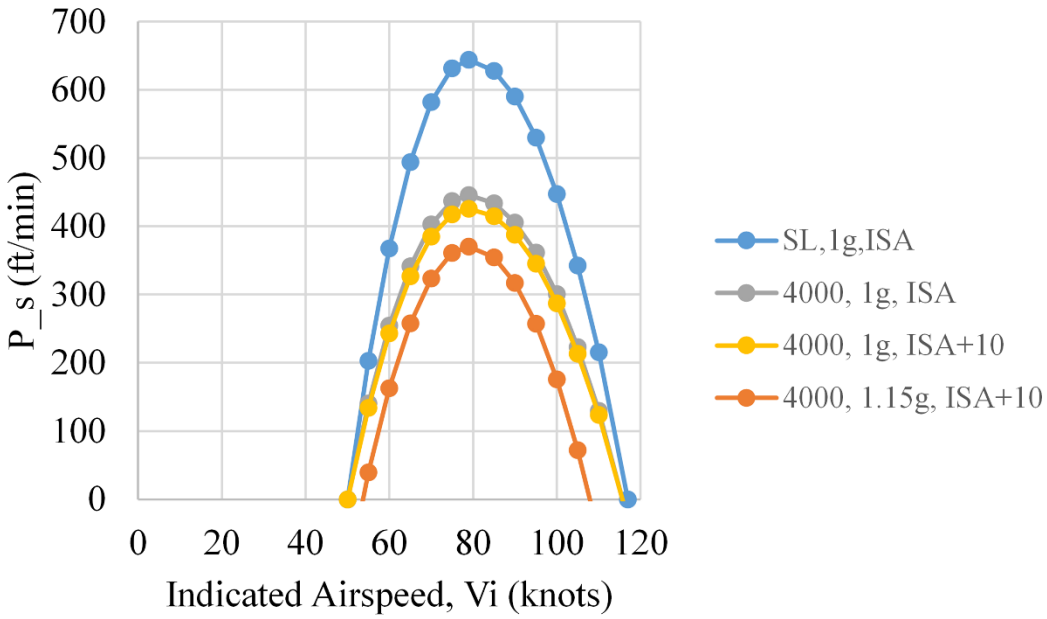

Figure 11. Sample P_S

5 Prototype displays

The team developed two types of engineering displays and one production display for use with the power and energy algorithms. One is a P_S display designed to be used by the pilot to fly around optimum performance point and to maintain flight with positive P_S reserves. The second display is an energy display, presenting the pilot with information about current and predicted energy states, along with warnings and instructions. The third, production display, merged

energy awareness data with primary flight data to provide the pilot with information and cueing while piloting an aircraft.

5.1 P_S display

The prototype P_S engineering display is illustrated in Figure 12. The display has two parts. The arrow in the left clock display shows the instantaneous P_S calculated from instantaneous altitude h and indicated airspeed V_i data, along with $\dot{h}$ and $\dot{V}_i$ calculated as discrete derivatives. The clock display is normalized over the maximum possible sustainable $P_{S,max}$, which is the maximum rate-of-climb at sea level, with wings level, at $n_z = 1\ g$. The right clock display shows the P_S envelope, again normalized over $P_{S,max}$. The gray shaded area indicates the safe P_S envelope, within which the aircraft is operated nominally. It is bounded on the upper end by the green line for the maximum available $P_{S_{avail}}$ for the current pressure altitude and air temperature, assuming $n_z = 1\ g$ and wings level. Therefore, the green line shows the available excess power reserves if the pilot levels the wings out and climbs at V_y. The lower bound of the safe P_S envelope is shown by the red-white limit line, showing the achievable $P_{S_{avail}}$ if the aircraft is operated at its current airspeed, but with 60° bank, which is considered the limit of the safe operating envelope. Within the gray envelope, there is a yellow line. The yellow line indicates the achievable $P_{S_{avail}}$ for the current indicated airspeed, the current n_z, and the current bank angle. By the width of the safe P_S envelope, the pilot can see whether the aircraft is flying in a safe state with adequate reserves. The narrower the envelope gets, the less P_S and hence acceleration potential or climb potential is available. For a tight turn at altitude, the green upper limit and the dashed lower limit will eventually meet, showing that the aircraft is about to stall.

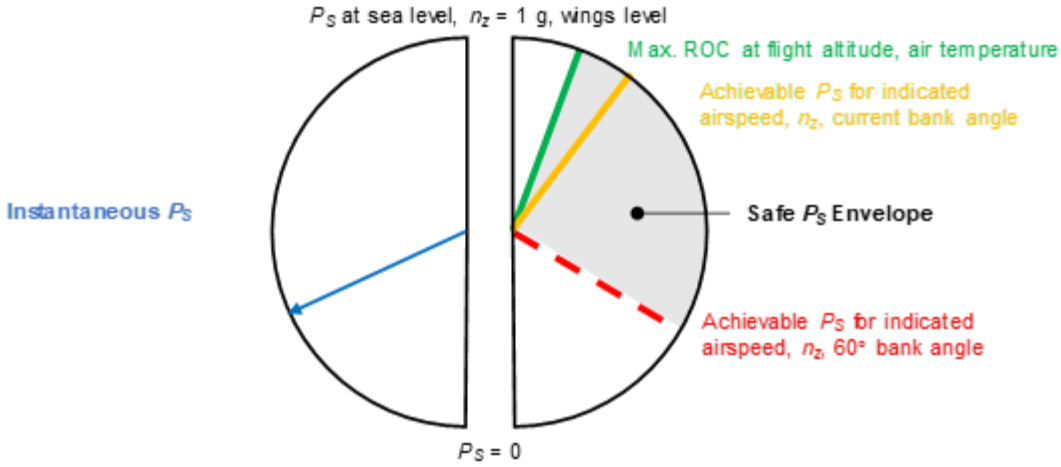

Figure 12. P_S Engineering display

5.2 Total energy display

The prototype display for total energy is illustrated in Figure 13. The total energy is indicated by a box, where the width represents the specific kinetic energy reserve, $\varepsilon_{kin,res}$, and the height represents the specific potential energy reserve, $\varepsilon_{pot,res}$. In light GA aircraft, $\varepsilon_{kin,res}$ is typically significantly smaller than $\varepsilon_{pot,res}$. Therefore, the width of the total energy boxes is scaled up by a factor of 15. The display shows three energy boxes. The red box indicates the minimum safe potential and kinetic energy thresholds. In this project, the minimum safe $\varepsilon_{pot,res}$ was set to 500 ft, the airspeed for minimum safe $\varepsilon_{kin,res}$ was 1.1 V_{S1}. The blue energy box is the predicted energy state based on the current potential and kinetic energy. The predicted kinetic energy assumes that 100% of the current P_S is turned into kinetic energy. The predicted potential energy assumes that the current P_S is completely turned into climb rate. The prediction horizon is arbitrary but should be set to accommodate the typical response time of a GA pilot. In the flight tests for the present paper, the horizon τ was set to 10 s.

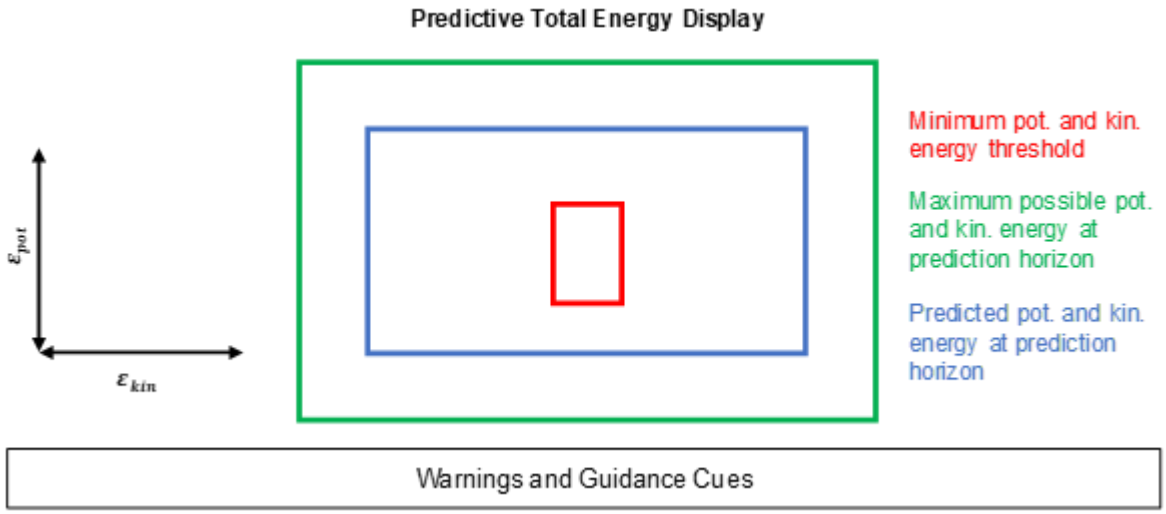

Figure 13. Engineering display for total energy

If either the kinetic energy or the potential energy side of the blue box sinks below the relevant energy threshold, the instantaneous energy box turns yellow, and warnings appear. If the potential energy is too low, the warning reads: "Too low. Climb." If the kinetic energy is too low, the warning reads: "Too slow. Push nose down." If both kinetic and potential energy cut below their thresholds, the instantaneous energy box becomes a solid red rectangle and the guidance cue "Wings level, nose level, accelerate to V_y and climb!" displays.

The green energy box shows the maximum possible kinetic and potential energy reserves at the prediction horizon. The size of the green box is calculated from the current potential and kinetic energy, and the maximum possible P_S at current altitude (wings level, $n_z = 1\ g$). The smaller the green box is, the less overall energy reserves the aircraft has.

5.3 Production display

A production display incorporating energy awareness information and pilot queuing based on total energy and required performance is illustrated in Figure 14. The energy awareness cueing is integrated into a heads up display presentation of primary flight data. The energy awareness algorithm adds energy and performance display elements as the total energy state of the aircraft becomes increasingly critical. Each element remains hidden until it earns its way onto the display as the information becomes relevant to the pilot. The presentation of energy awareness information is driven by the energy management algorithm, which predicts aircraft performance available and adjusts acceptable performance limits based on the total energy state of the aircraft.

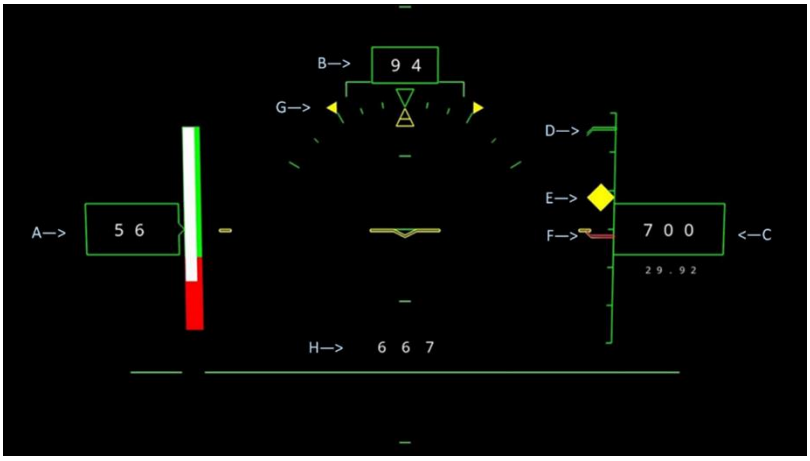

Figure 14. Production display showing primary flight data and energy awareness data:

A. Indicated Airspeed.
B. Heading.
C. Baro Corrected Altitude (MSL)
D. Energy-Maximum Available P_S.
E. Energy-Index, Current P_S.
F. Energy-Index, Minimum Acceptable P_S.
G. Energy-Roll Limit Index.
H. Geometric Altitude (AGL).

In addition to the standard primary flight data, the production display includes an energy index with three elements that show the pilot the current P_S, maximum available P_S, and minimum acceptable P_S for the current total energy state of the aircraft. The display also shows the aircraft's geometric, height above ground level (AGL), altitude, and roll limit index marks that indicate the maximum bank angle possible while still able to maintain the minimum P_S.

Three different display schemes were tested for the production display: (1) fully decluttered display with energy symbols only earning their way on to the display as prescribed by the energy state of the aircraft, (2) live primary flight information presented on the HUD with the energy symbols appearing as prescribed by the energy state of the aircraft, and (3) primary flight data and energy symbols that are always visible.

With the fully decluttered display, the evaluation pilot found the blank HUD combiner to be a nuisance. It was noted that the pilot tended to look around the combiner, moving his head away from the HUD eye box. Also, during one test in low visibility, the pilot commented that his eyes were focusing naturally on the combiner itself when symbols appeared in the collimated display; it required a focus shift before the symbols were clearly noticeable.

With primary flight information always displayed, the pilot remained focused on the HUD display and noticed the energy symbols come alive immediately.

It was noted during flight testing that the display itself is inadequate to attract the pilot's attention to a critical energy state. An audio warning or other prominent warning light could be paired with the information on the display to produce a more effective alerting system.

6 Energy awareness system

The energy awareness system (EAS) uses sensor data Air Data/Attitude Heading and Reference System (ADAHRS)/GPS, an aircraft performance model (APM), an energy margins model (EMM), and an energy awareness algorithm (EAA) to drive an energy awareness and alerting display. The EAS receives the data listed in Table 1 from the aircraft avionics bus to determine the aircraft's current total energy state and to predict the aircraft's maximum available performance in the form of excess P_S. The aircraft's total energy state is determined relative to geometric altitude and pilot queuing is triggered by limits determined using the EMM, which is based on the "energy funnel" concept presented above. As the total energy state becomes more critical, the limits for acceptable excess P_S become more constrained. The constraints on aircraft maneuvers required to maintain an acceptable energy margin are presented to the pilot in the form of bank angle cues and min/max acceptable P_S markers.

Table 1. Data sources and update frequency.

Data	**Source**	**Rate**
Pitch	ADAHRS	10Hz
Roll	ADAHRS	10Hz
Heading	ADAHRS	10Hz
Normal Accel	ADAHRS	10Hz
Lateral Accel	ADAHRS	10Hz
Rate of Turn	ADAHRS	10Hz
Indicated Airspeed	ADAHRS	10Hz
Pressure Altitude	ADAHRS	10Hz
Vertical Speed	ADAHRS	10Hz
Static Air Temperature	ADAHRS	10Hz
Baro Altimeter Setting	ADAHRS	10Hz
Latitude	GPS	25Hz

Data	Source	Rate
Longitude	GPS	25Hz
Groundspeed	GPS	25Hz
Groundtrack	GPS	25Hz

The Energy Awareness System requires the following five input elements:

1. **Air Data/Attitude Heading and Reference System (ADAHRS)** Prefiltered data is collected, at 10Hz from dual Garmin G5 Flight Instruments. Static air temperature and magnetic heading are provided through the G5 databus by an external line replaceable unit (LRU).
2. **Global Position System (GPS)** Position data is collected at 25Hz from two independent Wide Area Augmentation System (WAAS) GPS receivers. The two receivers are placed on the airframe with a known baseline to allow for simple differential GPS position correction.
3. **Shuttle Radar Topography Mission (SRTM) Database:** The geometric altitude is determined via reference to the SRTM 1 arc second data set. The data are resident in the working memory of a central processing unit (CPU) and provide the terrain elevation above mean sea level for the latitude and longitude of the aircraft. The energy awareness algorithm uses the geometric altitude to calculate the aircraft's total energy relative to the local surface reference and to determine when the aircraft is entering a low energy regime where it is appropriate for the energy display to place restrictions on the aircraft maneuvering envelope.
4. **Energy Margins Model (EMM):** The EMM defines the acceptable energy envelope, or "energy funnel," by setting the energy limitations on the display, and setting limits which affect both the appearance and behavior of energy symbols. The EMM also defines the trigger point for pilot cues when approaching critical energy states. Limits within the EMM divide determines green (normal), amber (caution), and red (warning) zones within the energy envelope, with each zone corresponding to a change of symbol color on the energy awareness display. The EMM must be explicitly defined for each aircraft and application.
5. **Aircraft Performance Model (APM)** The model is explicitly defined for each aircraft type. To implement the APM, the performance data derived from the aircraft POH, and flight test is converted to a lookup table indexed by V_i, h_p, ϕ, n_z, and T. The APM generates the P_S for the given input variables. The APM can be fed live

data to determine the aircraft's real time performance capability and can also be used to determine potential performance capability at any other point within the model's parameter space. The APM is referenced using defined input parameters to populate the limit markers of the energy index and to define the minimum P_S limits required to remain within the EMM performance margins.

6. **Energy Awareness Algorithm (EAA)** The energy awareness algorithm compares actual aircraft flight parameters from sensor data to the predicted aircraft performance and then determines the aircraft's state within the EMM. It determines the criticality of the energy state based upon the constraints specified in the EMM and populates display elements.
7. **Energy Awareness System (EAS):** Figure 15 illustrates the relationship between system elements. The information is collected by the input channels and fed into the energy awareness algorithm in real time with no filtering latency.

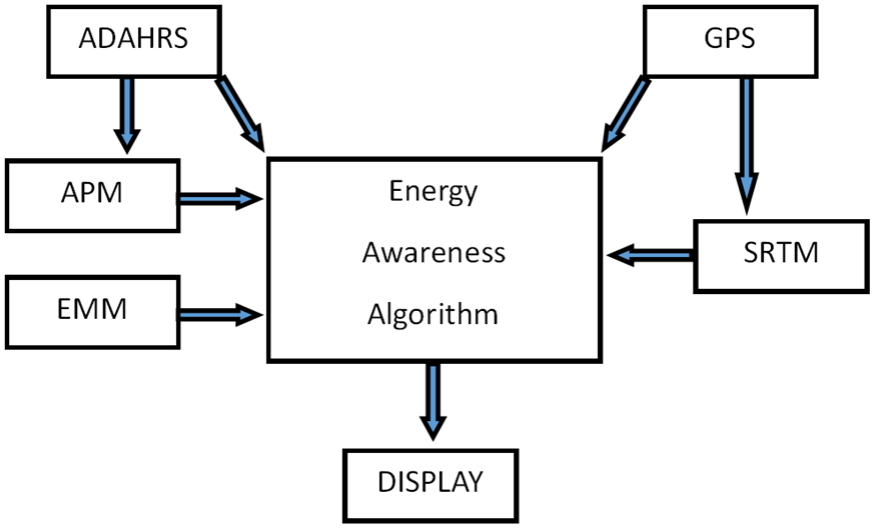

Figure 15. Major system components of the EAS

For the test flights, the EMM and EAA were coded to follow a scheme based on four altitude and airspeed regimes:

High Altitude/High Airspeed

- Above 1500’ AGL.
- The display shows primary flight data only.
- Energy awareness display is hidden.

High Altitude/Low Airspeed

- Above 1500’ AGL.
- Indicated airspeed below V_y, corrected for n_z.
- The display shows primary flight data and,
- The energy index appears on display without min P_S constraint.

Low Altitude

- The display shows primary flight data and,
- Below 1500’ AGL, the energy index is visible at all airspeeds.
- Below 1000’ AGL, the AGL altitude display becomes active.
- From 500-1500’ AGL, the minimum acceptable P_S becomes more constrained as altitude decreases.
- Bank angle limit markers display to cue the pilot to remain in the acceptable performance envelope if the energy drops into the yellow or red zone.

Critical Altitude

- The display shows primary flight data and,
- Below 500’ AGL, the energy index minimum P_S limit is set to produce a gradient of 200’/nm at the current speed .
- Bank angle limit markers display to cue the pilot to remain in the acceptable performance envelope if the energy drops into the yellow or red zone.

See Appendix A for a graphical depiction of display behavior.

7 Flight test

Two flight test programs were completed in both a Cessna 172N and a Piper PA-28-161, aircraft representative of common light general aviation aircraft.

The first flight test campaign had two objectives: (1) check and refine the POH-derived model for $P_{s_{avail}}$ and (2) fly the engineering display with live data. To accomplish the first objective, constant-speed climbs were performed at three airspeeds; one set at 1 g wings-level, and another set at $n_z = 1.15$ g. These two flights had ISA+20 conditions. The 1 g wings-level flight was flown using the standard constant-speed climb technique. The 1.15 g flight held speeds constant during a climbing turn at a constant bank angle of 30°. A Garmin G5 produced 1 Hz data for V_i, h_p, ϕ, n_z. Temperature was recorded from the standard probe in the pilot's windshield. Figure 16 shows a comparison of the model with the flight test data for 1 g, wings-level. The solid lines represent the model, and the individual points represent the flight test data. At 1,000 ft pressure altitude, the model matches the flight test data well. At 4,000 ft, the model is off by approximately 80 to 100 ft/min.

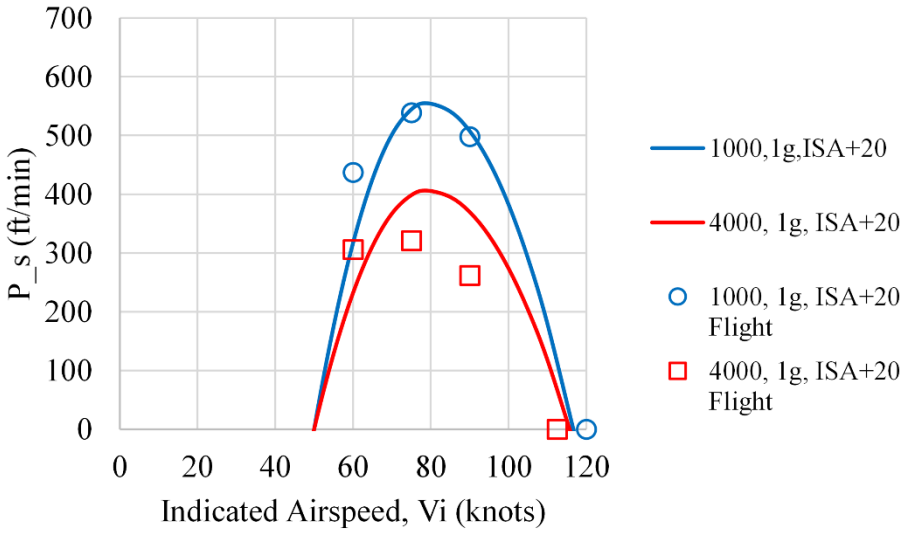

Figure 16. 1 g Comparison of model to flight test

Figure 17 shows a comparison of the model with the flight test data for 1.15 g. At 1,000 ft, the model is off by approximately 50 ft/min. At 4,000 ft, the model matches the flight test data well. As this was just a two-flight spot check of altitude and n_z effects, the model was deemed reasonable.

The third flight was conducted to better characterize an asymmetry in the observed performance between left and right hand coordinated turns during constant airspeed climbs. The actual P_S was significantly lower in coordinated turns to the right as compared to turns to the left. More control surface deflection of aileron, rudder, and elevator was required to hold coordinated turns to the right, resulting in increased drag and the decrease in performance. The effect was modelled in the energy management algorithm, but further flight test is needed to better quantify the effect.

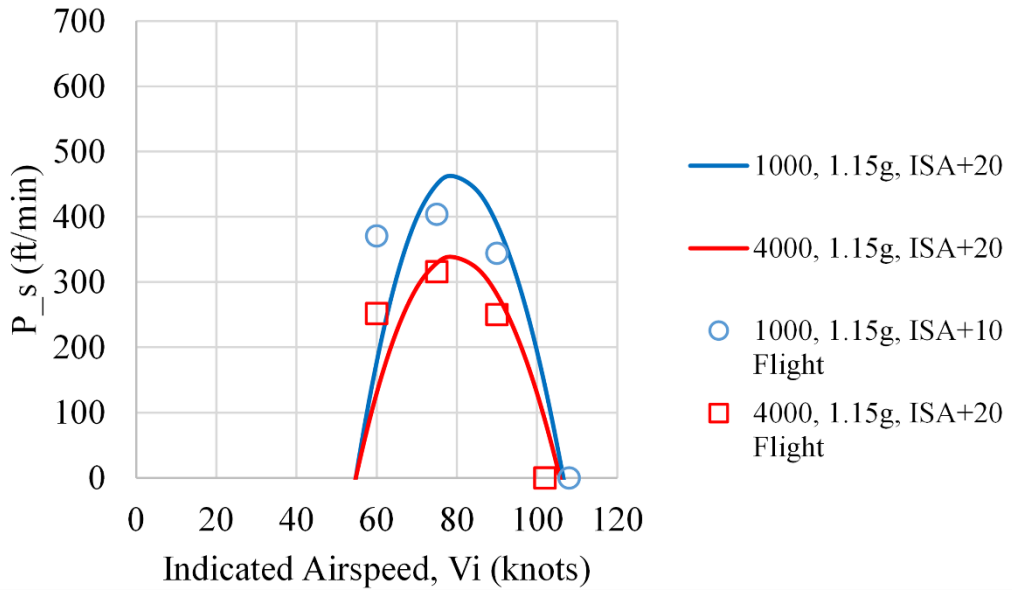

Figure 17. 1.15 g Comparison of model to flight test

The second flight test program had three objectives: (1) refine the performance of the energy awareness cues of the production display, (2) check the display for usability in the flight environment, and (3) qualitatively assess pilot experience when using the display. The flights were conducted in various visual conditions: day, night, low light, and low visibility. The aircraft performance model was left constant, and adjustments were made to the energy margins model.

Specific elements adjusted during the flights were display brightness, HUD eye box position, color selection, symbol size, and symbol shape. The prominence of the energy awareness elements was also adjusted as they earned their way on to the display in various phases of flight.

Three flights were conducted to test the usability of the display in flight in different conditions. The display was sunlight viewable during the day and the auto dimming feature on the HUD projector maintained the display at appropriate levels during dusk and night operations. The HUD eye box was large enough that the display was in the field of view in the normal seated pilot position in all phases of flight. The test pilot did not find the optical combiner or display to interfere with normal aircraft operations.

Three evaluation pilots conducted six flights with the production energy awareness display. Two different display modes were tested during the pilot assessment flights: decluttered display with energy awareness symbology only, and a primary flight information HUD display with energy awareness symbology. In both display modes, the energy awareness symbols were hidden until each element earned its way on onto the display. The pilots preferred the presentation with live primary flight data.

8 Future work

The EAS developed for this work incorporates both an aircraft performance model and an energy margin model. Combined with live flight data and the SRTM database, it is possible to predict potential terrain conflict based on the aircraft's potential performance both in a maximum performance level climb and in maneuvering flight. The aircraft performance model can predict the decreases in performance that will occur as an aircraft climbs to higher density altitude and the effects of performance on coordinated turns. With this information, a performance potential, integrated throughout a climb with effects of turns included, can be calculated and compared to required total energy margin limits. With the addition of available wind and true airspeed data and GPS derived track and groundspeed, the climb potential can be based not just on P_S and rate of climb, but on the climb, gradient required.

To produce a ground collision avoidance function, it is possible to add a look ahead feature to the current energy management system. One approach would be to look ahead of the aircraft's flight path in the SRTM database and compare terrain clearance requirements to the aircraft performance model to predict not only imminent ground collision hazards but also when the required climb gradients are approaching the performance limits of the aircraft. Two pilot cues are:

- The system can trigger a warning alert to indicate that the pilot must execute a maximum performance climb due to a terrain conflict.

- The energy awareness display can indicate to the pilot the current P_S to produce the climb gradient needed to clear terrain obstructions ahead. One location for the cue would be an additional marker on the energy index. Limits specified in the energy margins model could be used to predict impending low total energy conditions ahead of the aircraft and alert the pilot with cues earning their way on to the display as the energy state becomes increasingly critical.

For this study, the EAS only uses instantaneous ADAHRS sensor values to determine the aircraft's aerodynamic energy state. However, trend and attitude rate data would allow the EAS to adjust the acceptable energy margins based on such factors as the quality of the air, or the smoothness of the control inputs. The system could also use rate data to produce warnings to alert pilots to low energy and unstable flight dynamics, increasing energy margins as needed when high rates are detected. Three axis accelerometer and rate data are available through the existing hardware.

Future work would focus on the design and implementation of the look ahead terrain conflict function into the EAS and development of appropriate display symbology and other appropriate cues. Also, the addition of attitude rates as a factor in determining appropriate limits in the energy margins model to predict impending loss of control more effectively.

9 Conclusions

Loss of control at low altitude in the traffic pattern is one of the main causes of fatal accidents in general aviation. A HUD for energy state and specific excess power can potentially remedy these types of accidents. As GA airplanes are not equipped to measure many dynamic parameters, the predictive energy HUD must be based on an algorithm running on a reduced set of parameters readily available from the current generation of light aircraft avionics. This paper discusses the challenges associated with designing a HUD for light GA aircraft and presents a research HUD tested in a Cessna 172N and a Piper Warrior. The paper also presents a definition of total, potential, and kinetic energy reserves, which are relevant for flight. A predicted specific energy reserve at a prediction horizon can be calculated using the specific excess power. The paper describes methods to derive the available specific excess power at different pressure altitudes, temperatures, and load factors from data readily available in Pilot Operating Handbooks. Furthermore, the paper presents prototype displays for specific excess power and predicted reserve energy and reports on preliminary flight test results.

This paper also describes an EAS that uses sensor data and performance models to drive a display that provides energy state information and cueing to the pilot. The system provides additional data over traditional flight instruments that may promote a better awareness of the overall energy state of an aircraft. Information and warnings based on both the current and predicted energy state of an aircraft may provide an additional tool to combat loss of control.

10 References

Amelink, M. H., Mulder, M., Van Paassen, M. M., & Flach, J. (2005). Theoretical foundations for a total energy-based perspective flight-path display. *The International Journal of Aviation Psychology, 15*(3), 205-231.

Atuahene, I., Corda, S., & Sawhney, R. (2011). Development and flight test of a real-time energy management display. *Aviation, 15*(4), 83-91. doi:10.3846/16487788.2011.648310

Calise, A. J. (1977). Extended energy management methods for flight performance optimization. *AIAA Journal, 15*(3), 314-321. doi:10.2514/3.63239

Hankers, R., Pätzold, F., Rausch, T., Kickert, R., Cremer, M., & Troelsen, J. (2009). *Safety aspects of light aircraft spin resistance concept.* Cologne: European Aviation Safety Agency.

Kish, B. A., Bernard, T., & Kimberlin, R. (2016). A limited investigation of airplane response to flap extension. *IEEE Aerospace Conference.* Big Sky, MT.

Kish, B. A., Wilde, M., Kimberlin, R. D., Sizoo, D. G., Mitchell, D. G., Peter, L., . . . Geehan, J. (March, 2018). FAA Part 23 methods of compliance for AOA warning/limiting systems. *IEEE Aerospace Conference.* Big Sky, MT.

Kish, B. A., Wilde, M., Kimberlin, R., Silver, I., Kolano, E., Schaller, R., . . . Webber, D. (June, 2018). Stall characterstics and trim changes of six general aviation aircraft. *AIAA Aviation Forum and Exposition.* Atlanta, GA.

Kish, B. A., Wilde, M., Kimberlin, R., Silver, I., Sizoo, D. G., Webber, D., . . . Toepfer, M. (2019). Trim forces and free response to configuration changes on general aviation aircraft. *IEEE Aerospace Conference.* Big Sky, MT.

Lambregts, A. A. (1983). Integrated system design for flight and propulsion control using total energy principles. *AIAA Aircraft Design, Systems and Technology Meeting.*

Lambregts, T., Rademaker, R., & Theunissen, E. (2008). A new ecological primary flight display concept. *27th AIAA/IEEE Digital Avionics Systems Conference.* St. Paul, MN. doi:10.1109/DASC.2008.4702820

Merkt, J. R. (2013). Flight energy management training: Promoting safety and efficiency. *Journal of Aviation Technology and Engineering, 3*(1), 24-36. doi:10.7771/2159-6670.1072

National Transportation Safety Board. (2011). *Review of U.S. civil aviation accidents 2007-2009.* Washington, DC: NTSB.

National Transportation Safety Board. (2019). *Data & stats.* Retrieved October 18, 2019, from https://www.ntsb.gov/investigations/data/Pages/Data_Stats.aspx

Piper Aircraft Corporation. (1994). *Archer III pilot's operating handbook and FAA approved airplane flight manual.* Vero Beach, FL: Piper Aircraft Corporation.

Rutowski, E. S. (1954). Energy approach to the general aircraft performance problem. *Journal of Aeronautical Sciences, 21*(3). doi:doi.org/10.2514/8.2956

Wu, S.-F., & Guo, S.-F. (1994). Optimum flight trajectory guidance based on total energy control of aircraft. *Journal of Guidance, Control, and Dynamics, 17*(2), 291-296. doi:10.2514/3.21196

Zagalsky, N. R. (1973). Aircraft energy management. *AIAA 11th Aerospace Sciences Meeting.* Washington, DC. doi:10.2514/6.1973-228

A Graphical depiction of display behavior

The figures below show the Energy Awareness System (EAS) display elements in various phases of maneuvering flight.

Figures A-1 through A-7 show the aircraft at various airspeeds and bank angles in a high altitude regime where the energy margins model provides limited constraints. The aircraft is free to maneuver with a surplus of total energy.

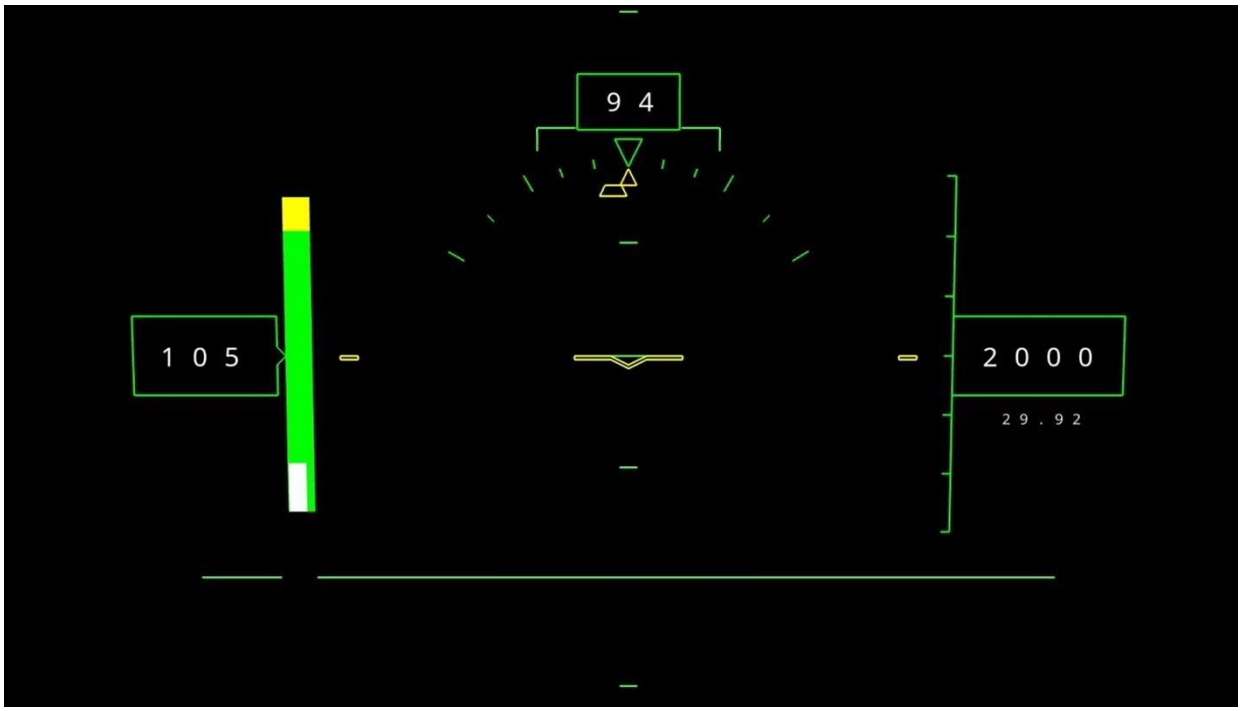

Figure A- 1. 2000 MSL, 1971 AGL, 105 Knots Indicated Airspeed (KIAS). The energy cues are not visible.

Note that the max Ps (green line) and min acceptable Ps (red line) will box the limits of our defined “energy funnel.” The diamond represents current Ps based upon IAS, density altitude, load factor/bank angle and the performance model of the aircraft.

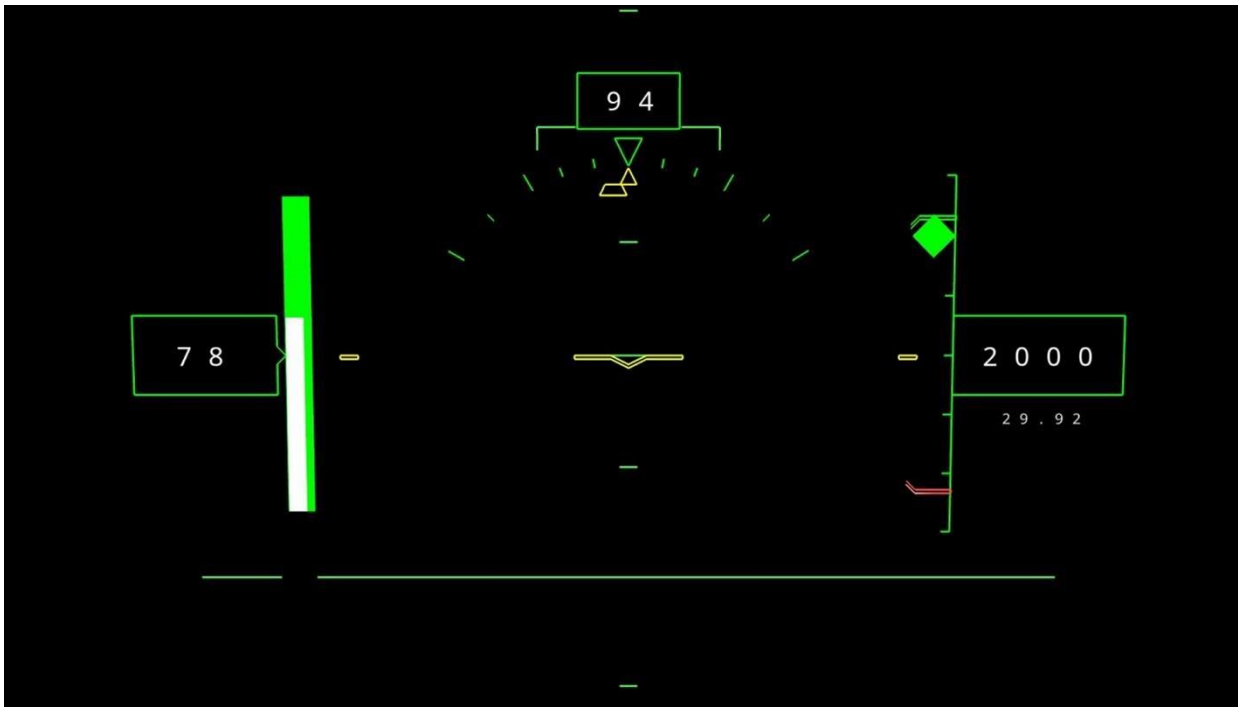

Figure A- 2. Aircraft Slowing, 2000 MSL, 1971 AGL, 78 KIAS. The energy cues come alive as the aircraft drops through Vy . This happens at any altitude.

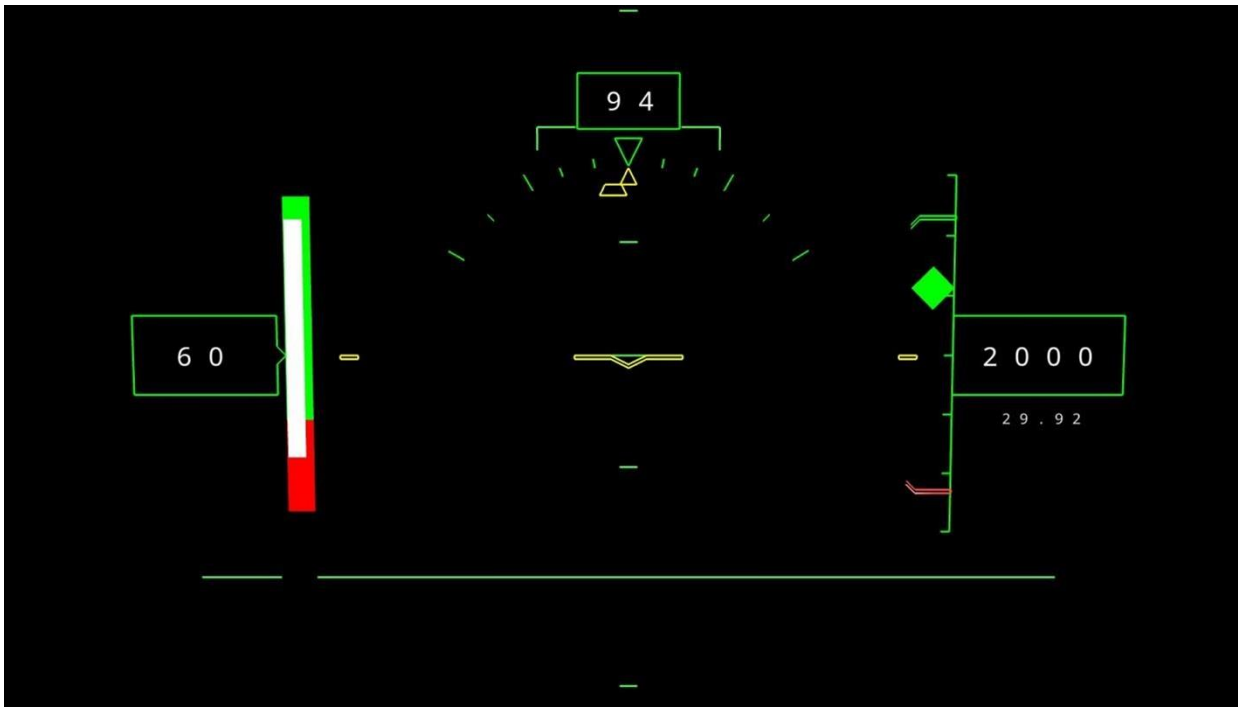

Figure A- 3. The aircraft slows below Vy.
The diamond Ps indicator begins to move down the index.

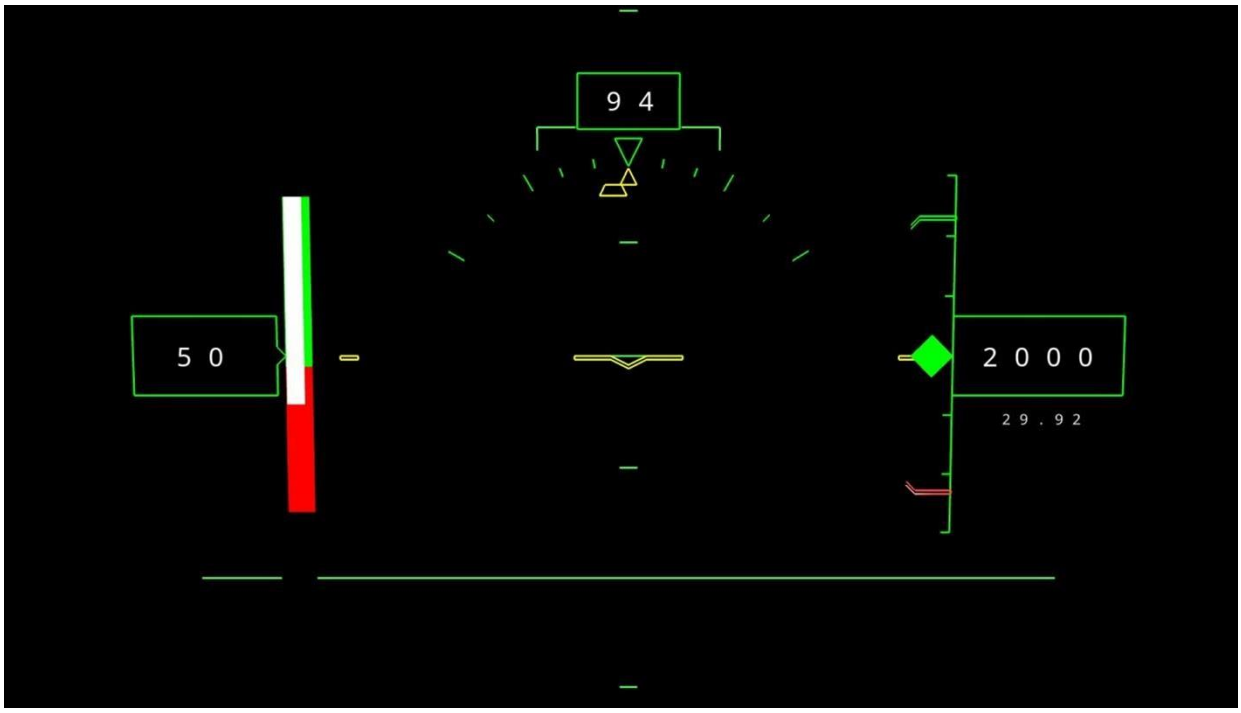

Figure A- 4. The aircraft slows to 50 knots.
At this density altitude the performance model predicts $Ps{\sim}zero$. The green line still represents max available Ps at this density altitude.

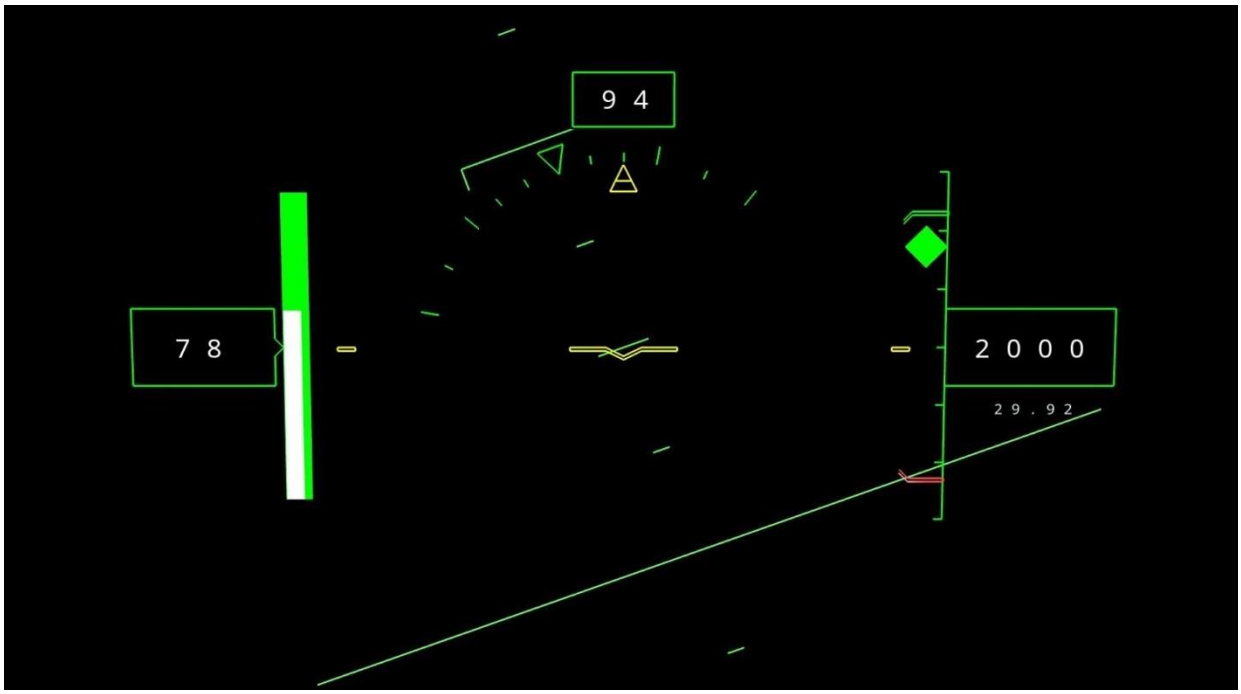

Figure A- 5. The aircraft is at 78 knots, in a 20 degree bank.
The diamond *Ps* indicator decreases accordingly.

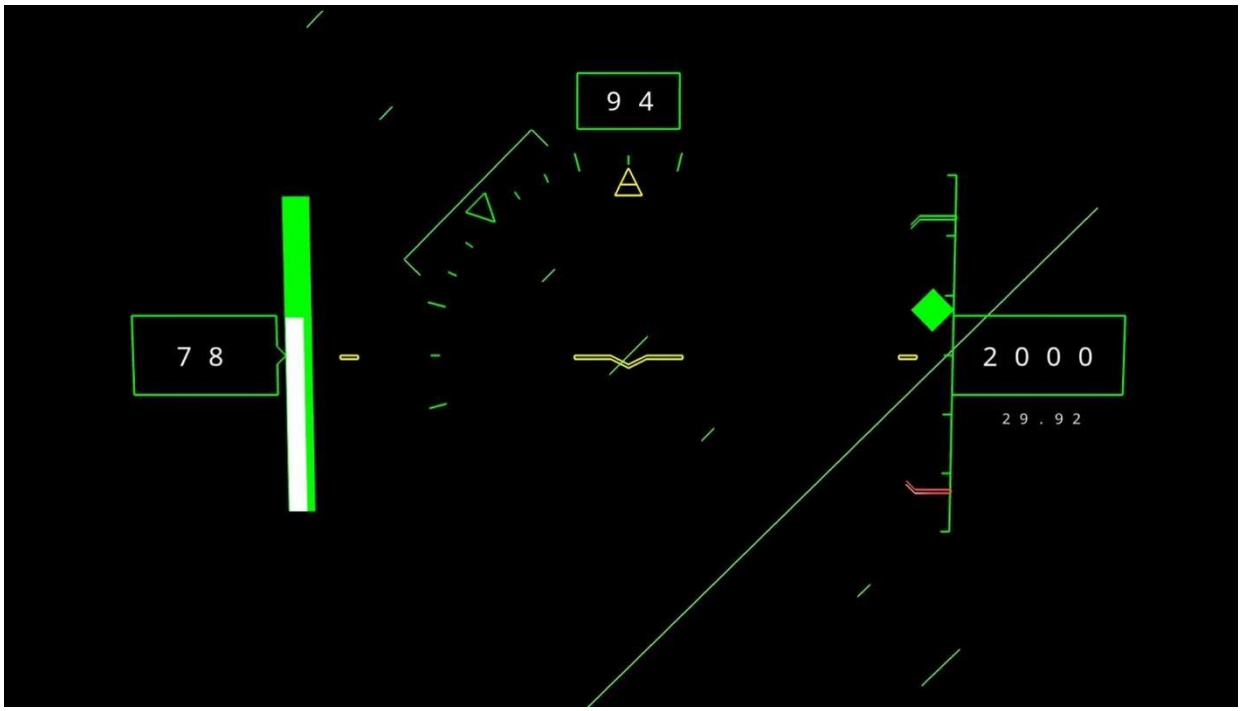

Figure A- 6. Airspeed 78 KIAS, 45 degree bank. The diamond *Ps* indicator decreases accordingly.

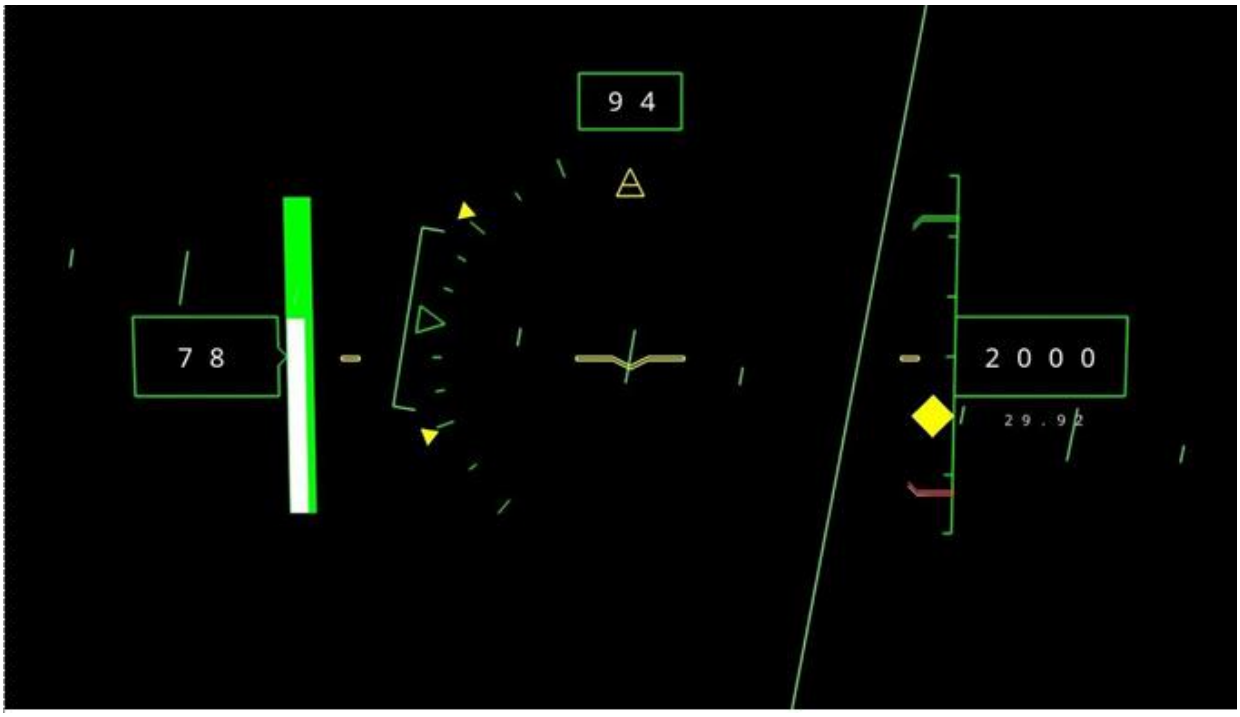

Figure A- 7. Airspeed 78 KIAS, 80 degree bank. The *Ps* has dropped into a caution range for this total energy state. The *Ps* cue changes to caution yellow and a target bank angle range is depicted on the roll index

Figures A-8 through A-15 depict a descent from an altitude without energy constraints to a low altitude on a simulated final approach to land.

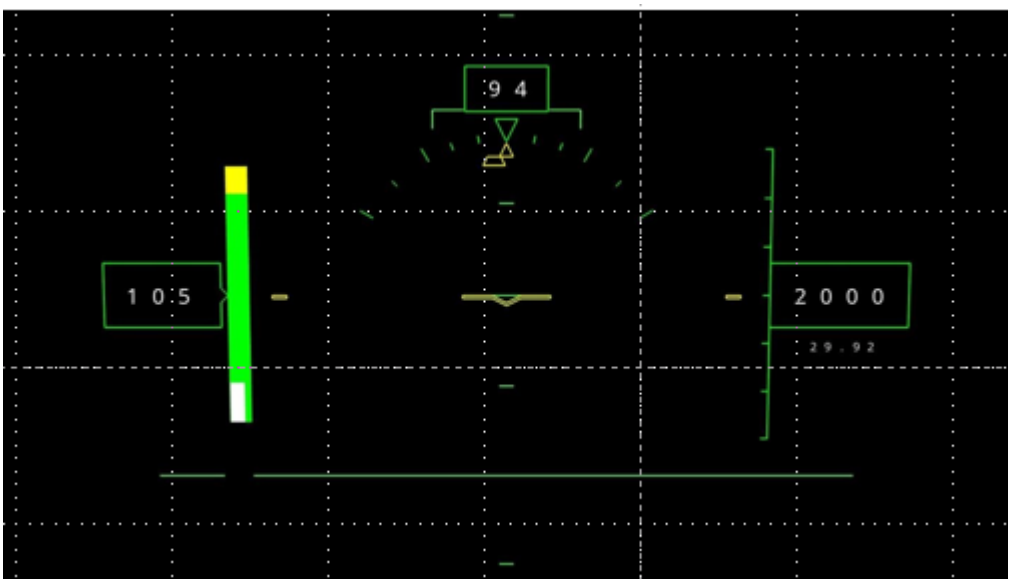

Figure A- 8. Airspeed 105 knots, level, 2,000 MSL, 1971 AGL.

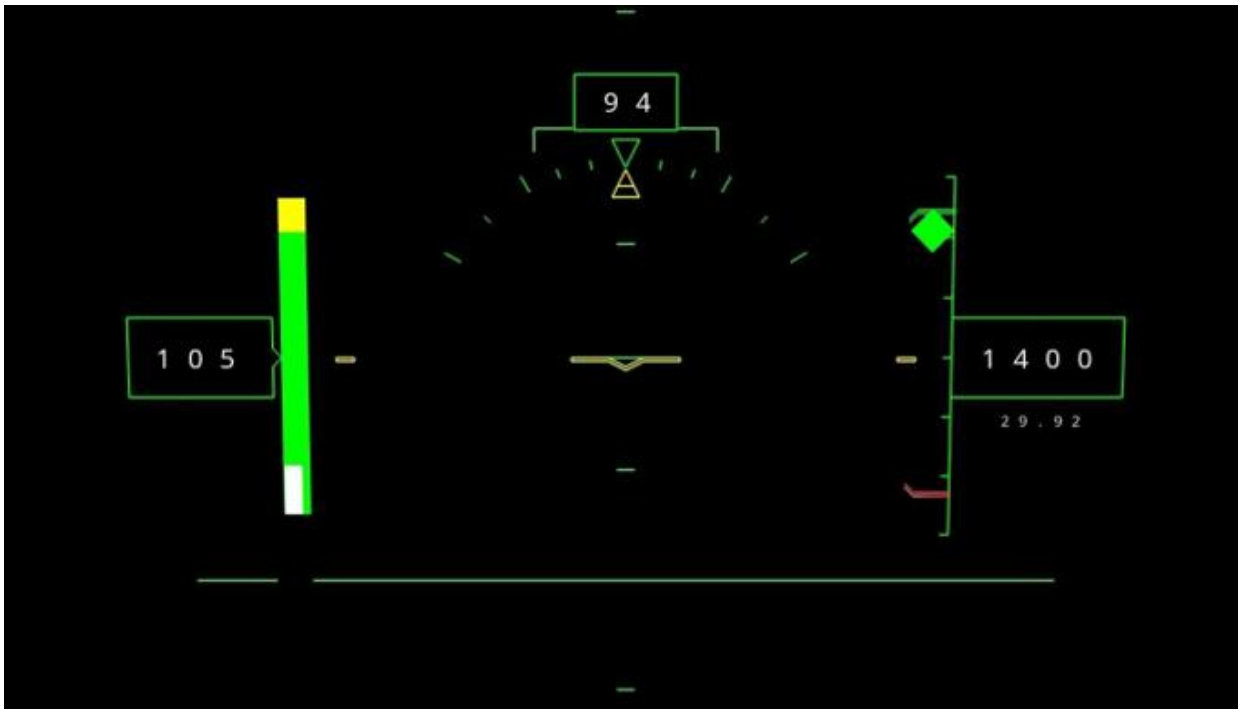

Figure A- 9. The aircraft descends through 1500 AGL, the energy index comes alive on the right side of the HUD.

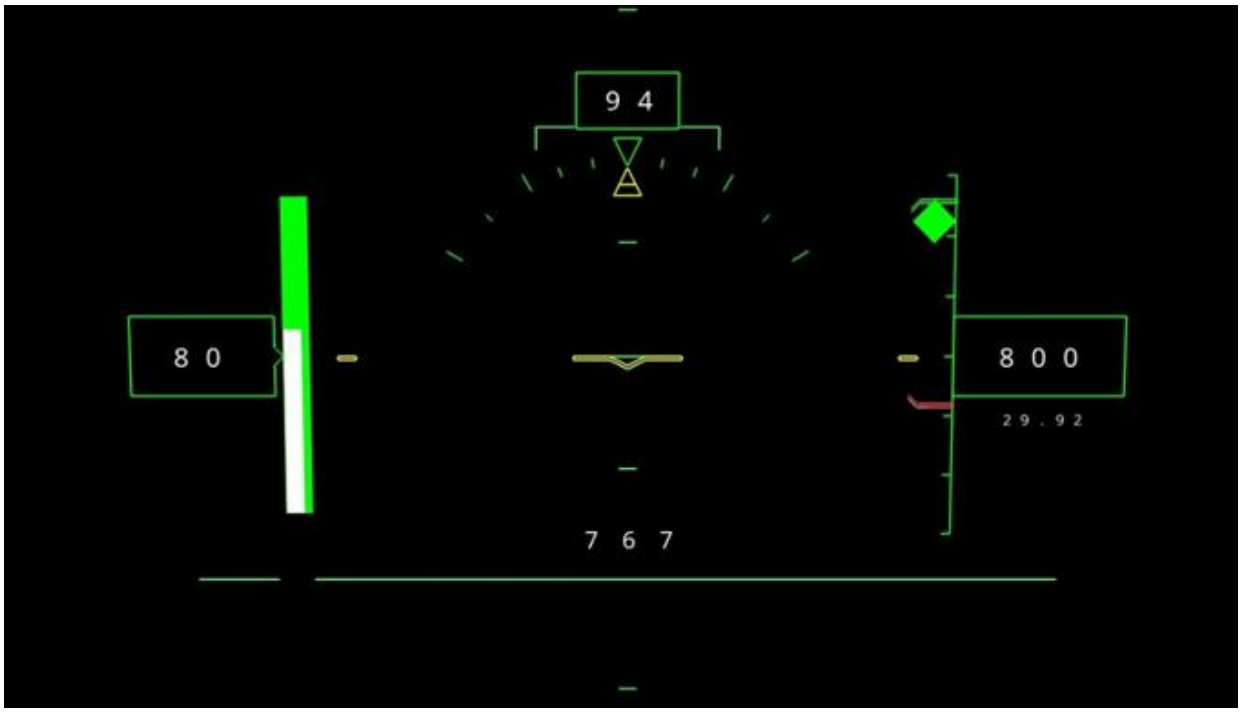

Figure A- 10. The aircraft descends below 1000 AGL and begins slowing to approach speed. Note that the red min acceptable Ps limit line has changed further.

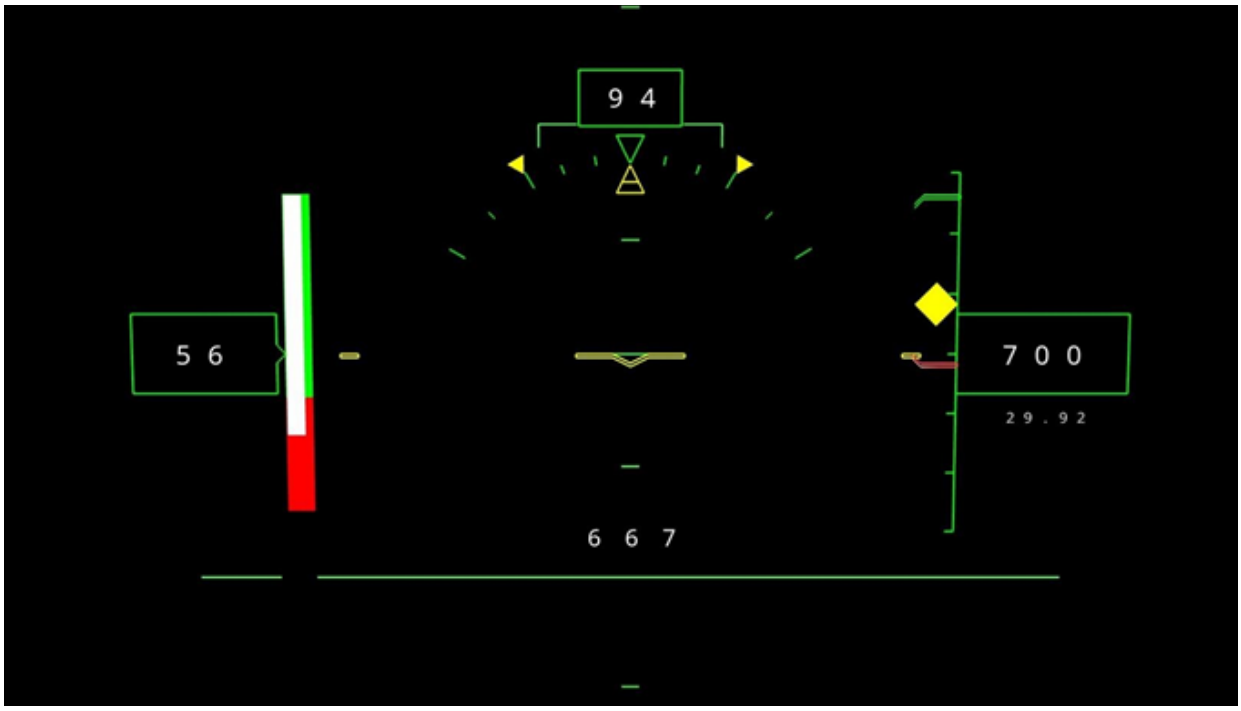

Figure A- 11. The pilot has allowed the airspeed to decay. It is now below the optimum level of 63 KIAS. The *Ps* cue changes to caution yellow and roll index limits appear. The roll index limit represents a bank angle, resulting in the minimum allowable *Ps*.

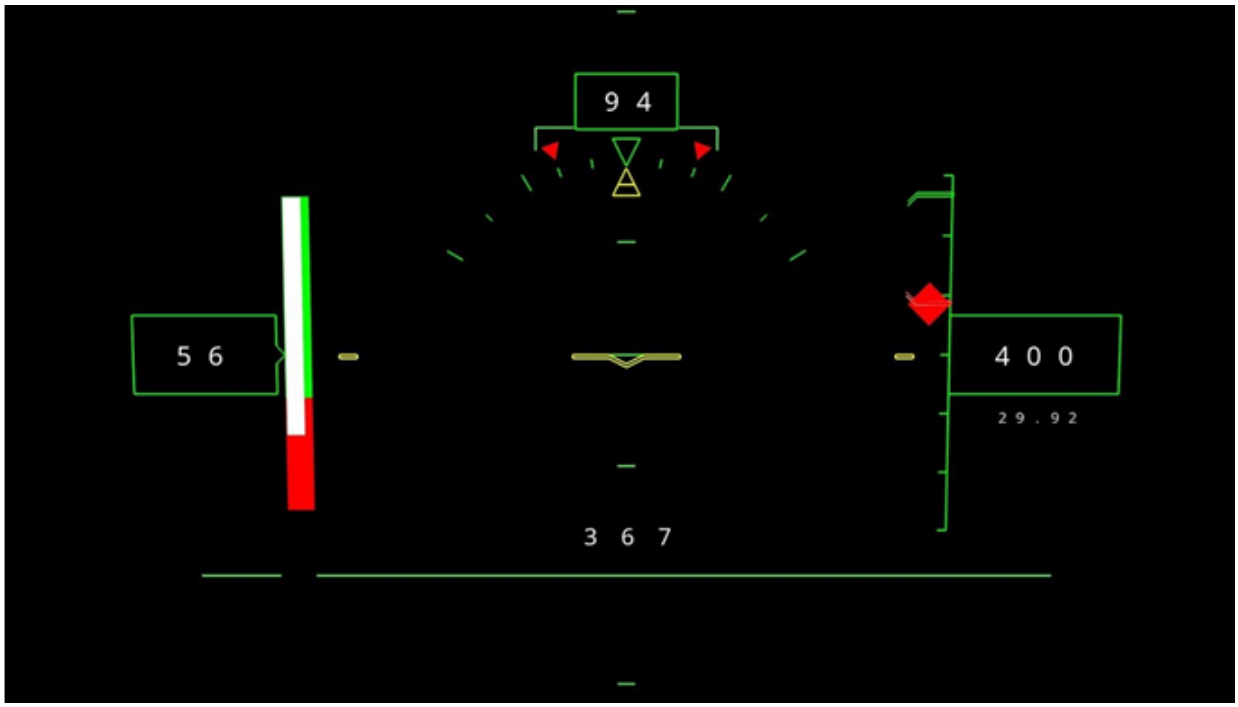

Figure A- 12. The pilot continues under 400 AGL with inadequate airspeed. At this point, the plane has entered a state where the airspeed is too low to meet the minimum allowable Ps at this total energy state.

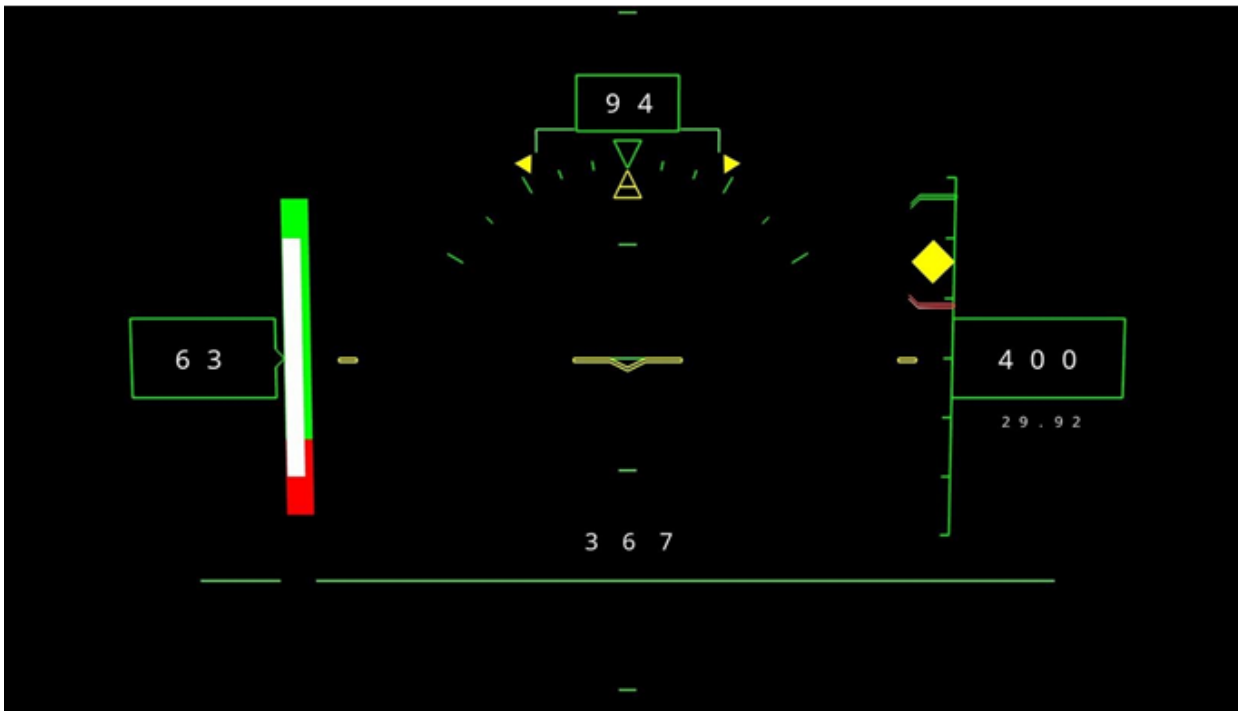

Figure A- 13. The pilot corrects and returns to an acceptable approach speed that will produce at least the minimum allowable *Ps* for this energy state.

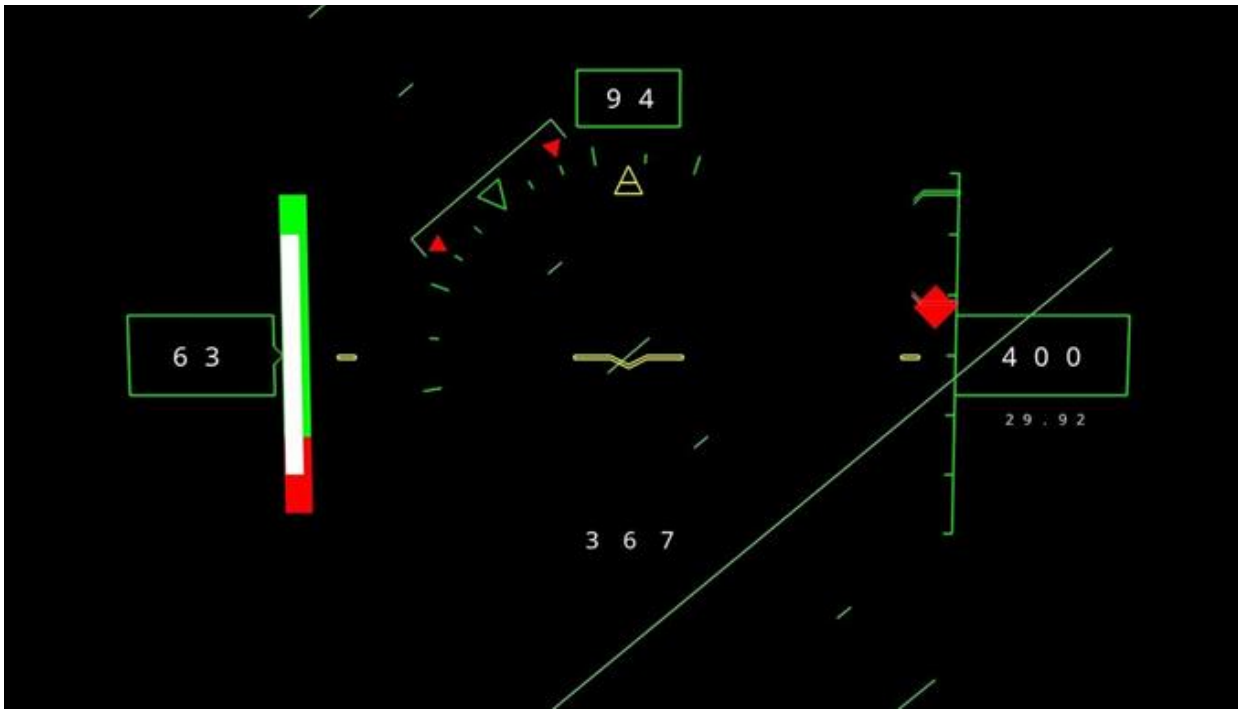

Figure A- 14. The pilot initiates a maneuver at low altitude that produces an unacceptable energy state. The airspeed will need to be increased or the bank angle returned to the acceptable envelope to return to the inside of the “energy funnel.”

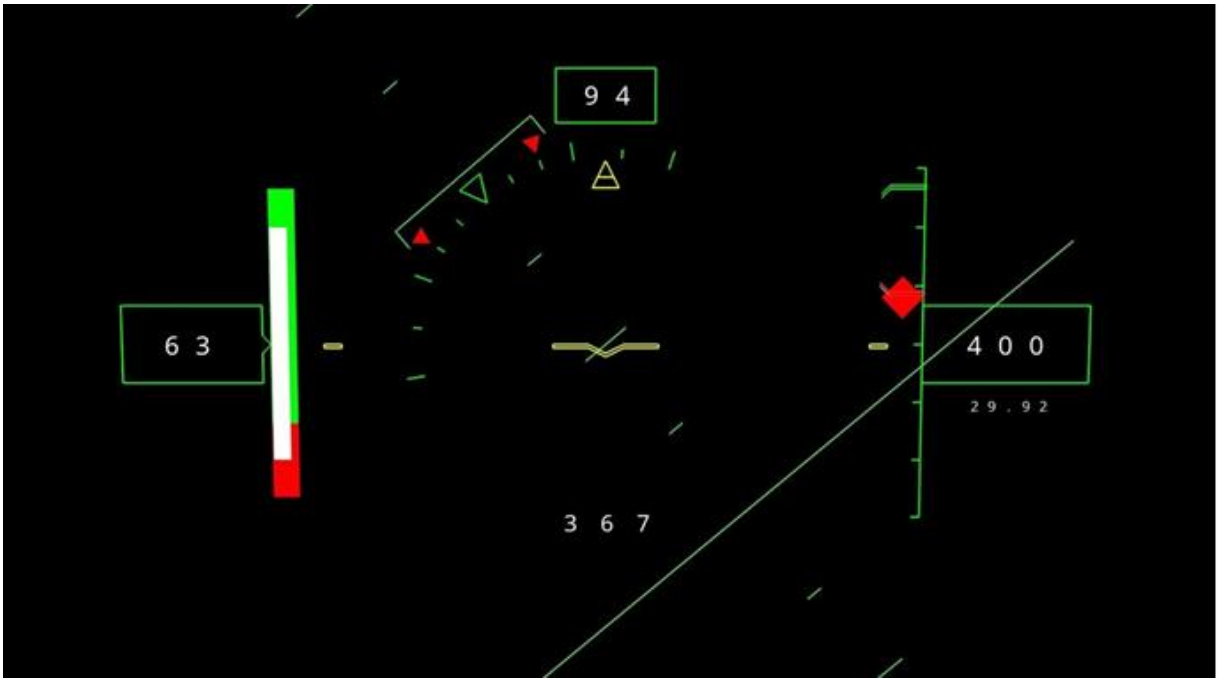

Figure A- 15. The pilot initiates a maneuver at low altitude that produces an unacceptable energy state. The airspeed will need to be increased or the bank angle returned to the acceptable envelope to return to the inside of the “energy funnel.”